Table 1 Clinical features and mutation characteristics of the MDS/AML patients with AML1 mutations

Case no.	*Age (years)/ sex*	*Diagnosis*	*History of exposure*	*Chromosome*	*AML1 mutation*	*Other mutations*
3	69/M	RAEBt	A-bomb (2.7 km)	Others	G42R	
4	59/F	RAEBt	A-bomb (1.7 km)	Others	L71fsX94	N-RAS(G60E) SHP2(N58Y)
5	68/M	RAEBt	A-bomb (0.8 km)	−7, others	D171N	N-RAS(G13D)
6	80/F	AML following MDS	A-bomb (2.5 km)	+8	G42R	
7	80/M	RAEBt	Mustard gas	Normal	Y113X	
8	43/F	RAEBt	AML(M3); Chem	−7	D171N	N-RAS(G12V)
9	39/F	RAEBt	Astrocytoma; Rad/ Chem	7q-	R177Q	
16	74/M	AML following MDS	—	Normal	S114fsX119	
17	65/M	RAEB	—	+8	R130fsX148	
18	47/F	RAEBt	—	Normal	R142fsX151	
19	79/M	RAEBt	—	7q-, +8	G143_K144insRRG	
20	64/F	RAEB	—	Normal	I166T	N-RAS(Q61K)
21	75/M	RAEBt	—	−7	D171G	FLT3(ITD 7aa) SHP2(F71L)
22	41/M	RAEB	AML(M5b); Chem	Others	T84_L85insP	
23	62/M	RAEBt	Esophageal cancer; Rad	Others	V137_G138insG	
24	62/M	AML following MDS	—	Normal	A224fsX228	SHP2(A72T)
25	75/M	RAEBt	—	+8	P232fsX567	SHP2(N58Y)
26	73/M	RAEBt	—	−7	D242fsX287	
27	55/F	AML following MDS	—	Normal	S291fsX300	
28	75/M	AML following MDS	—	Normal	R292fsX574	NF1(S382fsX390)
29	70/F	RAEBt	—	−7	T296fsX305	FLT3(ITD 7aa)
30	54/M	RAEB	—	Normal	T296fsX338 T296Sins(36aa)	
31	64/M	RAEB	—	7q-, +8	A364fsX570	
32	87/F	RAEBt	A-bomb (2.0 km)	Normal	L378fsX573	
33	65/F	AML following MDS	—	+21	D171N	
34	83/M	RAEB	—	Normal	G172R	
35	76/M	AML following MDS	—	Others	Q247fsX283	
36	71/F	RAEBt	Thyroid cancer; Chem	Normal	P248fsX283	N-RAS(G13D)
37	80/M	RAEB	—	Normal	S266fsX288	
38	68/M	RAEB	—	Normal	Y322fsX569	NF1(C118fsX164)
39	63/F	RAEBt	A-bomb (2.5 km)	+8	G340fsX576	FLT3(ITD 22aa)
40	64/M	RAEB	—	Normal	Y379fsX573	
41	66/M	AML following MDS	—	Normal	G394fsX562	FLT3(ITD 11aa)
42	72/M	RAEB	A-bomb (1.1 km) AML(M5); Chem	7q-, +8	R396_P398del	

AML = acute myeloid leukemia; MDS = myelodysplastic syndrome; RAEB = refractory anemia with excess blast; RAEBt = RAEB in transformation. A-bomb indicates atomic bomb, and distances in parentheses indicate how far from the center of the explosion the patient was. Chem = chemotherapy; Rad = radiation therapy.

Most chromosomal aberrations were unbalanced numeric alterations, including partial and complete chromosome loss or chromosome gain, in both groups of patients. −5/5q- was found with a significantly higher frequency in the AML1-wild-type group compared with the AML1-mutated group (17/80 versus 0/34, $P=0.0027$), but no significant association was observed between AML1 mutations and −7/7q-, 20q- or +8. However, half of the patients with a complex karyotype had more than 10 aberrations, and many of them had both −5/5q- and −7/7q- abnormalities. Therefore, we compared the incidence of −7/7q- with a normal chromosome 5 between AML1-mutated patients and AML1-wild-type patients (Table 2). This 'simple' −7/7q- abnormality was seen in nine (26%) of the 34 patients with AML1 mutations, and in three (4%) of the 80 patients without AML1 mutations ($P=0.0009$). Of the four patients with AML1-mutated MDS/AML (cases 8, 9, 22 and 42) who had a history of treatment with alkylating agents, three patients presented the −7/7q- cytogenetic abnormalities.

−7/7q- and N-RAS *mutation are closely related to AML1 mutations in patients developing MDS after chemotherapy for AML*

We identified two patients who developed MDS/AML with AML1 mutations after receiving chemotherapy for AML (Figure 1). At the point of AML diagnosis, they did not show AML1 mutations. Several years after they achieved complete remission, they developed MDS with AML1 mutations. Interestingly, the −7/7q- chromosomal abnormality and the *N-RAS* mutation also developed at the time of MDS diagnosis. One patient (case 8) had a history of receiving chemotherapy, including alkylating agents and all-*trans* retinoic acid, for AML (M3). This patient had a normal karyotype and a *PML-RARα* oncogenic chimeric gene. Continuous complete remission (CCR) was achieved for 3 years, and then she developed MDS (RAEBt). No mutation was found in either the *AML1* or the *N-RAS* gene before she developed MDS. At the time of MDS diagnosis, she had a karyotypic abnormality of monosomy 7. Moreover, she gained not only an *AML1* mutation but also an

Table 2 Cytogenetic abnormalities in MDS/AML patients with or without AML1 point mutations

Karyotype	*With AML1 mutation (N=34)*	*Without AML1mutation (N=80)*	*P-value**
Normal	15	33	0.8371
Simple karyotype[a]	19	27	0.0369
Complex karyotype[b]	0	20	0.0007
−7/7q- with normal chromosome 5	9	3	0.0009
−5/5q-	0	17	0.0027
20q-	1	7	0.4323
+8	7	13	0.5970
21 abnormality	1[c]	5[d]	0.6673

*Fisher's exact probability test was used to determine the *P*-value.
[a]Less than five aberrations.
[b]Five or more aberrations.
[c]A patient with trisomy 21.
[d]Patients including one case with +21, one case with +21q and three cases with balanced translocations with the break point of 21q22.

N-RAS mutation, and lost the *PML-RARα* chimeric gene. The other patient (case 42) had a history of atomic bomb exposure. He received chemotherapy including alkylating agents for AML (M4) with a t(2;11) karyotype. Continuous complete remission was achieved for 10 years, during which time he showed a normal karyotype. Then he developed MDS (RAEB) with an AML1 mutation with a karyotypic abnormality of 7q- and +8. At the time of MDS diagnosis, the t(2;11) clone was not detected.

Genetic abnormalities in MDS/AML patients with AML1 point mutation

To investigate the gene mutations in patients with MDS/AML or CBF leukemia, we analyzed the *N-RAS, K-RAS, PTPN11, NF1, FLT3, c-KIT* and *p53* genes (Table 3). We found a total of nine *N-RAS* mutations, four *PTPN11* mutations, two *NF1* mutations, eight *FLT3* mutations, six *c-KIT* mutations and 12 *p53* mutations. Two patients with an AML1 mutation had two additional mutations (*N-RAS* and *PTPN11, PTPN11* and *FLT3*). No mutation of the *K-RAS* gene was detected in these patients with MDS/AML or CBF leukemia. Activating *RAS* mutations, loss-of-function mutations in *NF1* and gain-of-function *PTPN11* mutations imply that there is upregulation of the RAS signaling pathway. Furthermore, activating mutations of *c-KIT* and *FLT3* also induce activation of the RAS signaling pathway. *N-RAS, PTPN11, NF1* and *FLT3* mutations were more frequent in AML1-mutated MDS/AML patients compared with AML1-wild-type MDS/AML patients (15 versus 3.8%, 12 versus 0%, 6.5 versus 0%, and 12 versus 2.5%, respectively), but not significant except for *PTPN11* ($P=0.0069$). However, the frequency of all these mutations affecting the RTK–RAS signaling pathway was significantly higher in AML1-mutated MDS/AML patients than in AML1-wild-type MDS/AML patients (38 versus 6.3%, $P<0.0001$). Conversely, *p53* mutations were not detected in the 34 patients with AML1 mutations, but were detected in 12 (15%) of the 80 patients without AML1 mutations ($P=0.0170$). Mutations in c-KIT were frequently detected in CBF leukemia patients, but were not detected in any of the patients with MDS/AML. Furthermore, similar to MDS/AML patients with AML1 point mutations, a high frequency (nine of 25, 36%) of RTK–RAS signaling pathway mutations was observed in patients with CBF leukemia.

SHP-2 mutants contribute to prolonged and enhanced extracellular signal-regulated kinase activation following stem cell factor stimulation

Somatic mutations in *PTPN11* are known to upregulate SHP-2 physiologic activation, leading to RAS pathway activation. This gain of function in mutated SHP-2 depends on ligand stimulation. Epidermal growth factor (EGF),[25,26] and granulocyte-macrophage colony stimulating factor (GM-CSF)[27] are known as ligands that upregulate mutated SHP-2, but so far SCF has not been known as such as a ligand. In AML1-mutated MDS/AML patients, genes involved in the RTK–RAS signaling pathway were frequently mutated, and blast cells of these patients expressed surface c-KIT (data not shown). Therefore, we suspected that cells bearing SHP-2 mutants would send strong stimulation signals through the RTKs, especially c-KIT. To investigate the effect of the mutant SHP-2 molecules on the RTK–RAS signaling pathway activation in response to SCF, we used HEL cells, which express the SCF receptor protein c-KIT. We established cell lines stably expressing Myc-tagged wild-type or mutant SHP-2 proteins (Figure 2). D61Y and E76K mutant SHP-2 proteins were previously identified in samples from patients with juvenile myelomonocytic leukemia (JMML), and their molecular characteristics have been thoroughly analyzed.[25,27,28] Cells were stimulated with SCF for various amounts of time, and we examined the activation of a downstream effector of RAS, extracellular signal-regulated kinase (ERK). Levels of phospho-ERK (p-ERK) at baseline were not elevated in cultures transduced with any SHP-2 constructs compared with parental HEL cells (compare lane 1 with lane 8 in Figure 2b). The HEL cells expressing wild-type SHP-2 showed activation of ERK at 5 min after SCF stimulation, a maximum activation level at 10 min, and p-ERK levels returned to baseline after 30 min. In cells expressing mutant SHP-2, SCF stimulation induced a prolonged and more intense signal of p-ERK lasting up to 60 min (Figure 2b, c). Although previous reports showed that the D61Y mutant was less hypersensitive than E76K in response to GM-CSF and IL-3,[27,28] our data showed that hyperactivity to SCF stimulation was detected slightly more in the D61Y-expressing cells than in the E76K-expressing cells (Figure 2b, c). The discrepancies between these studies and our data might be due to differences in the cytokine-dependent or independent cell systems and/or stimulating cytokines. The mechanism of different reactivities between these mutants is unclear, but may be caused by a minute structural difference.

Discussion

In this study, we have demonstrated correlations between AML1 point mutations and −7/7q- or gene mutations affecting the RAS signaling pathway in patients with MDS/AML (i.e., RAEB, RAEBt and AML following MDS). This correlation was also shown in the clinical course of two patients who developed therapy-related MDS/AML with a combination of an AML1 mutation, a −7/7q- abnormality and an *N-RAS* mutation induced by chemotherapy for AML (Figure 1).

Our study revealed a significant association between AML1 mutations and −7/7q-, and between normal AML1 and −5/5q- in both sporadic and secondary cases of MDS/AML patients. Previous studies have shown that the genetic pathways for development of MDS/AML may be classified by the cytogenetic

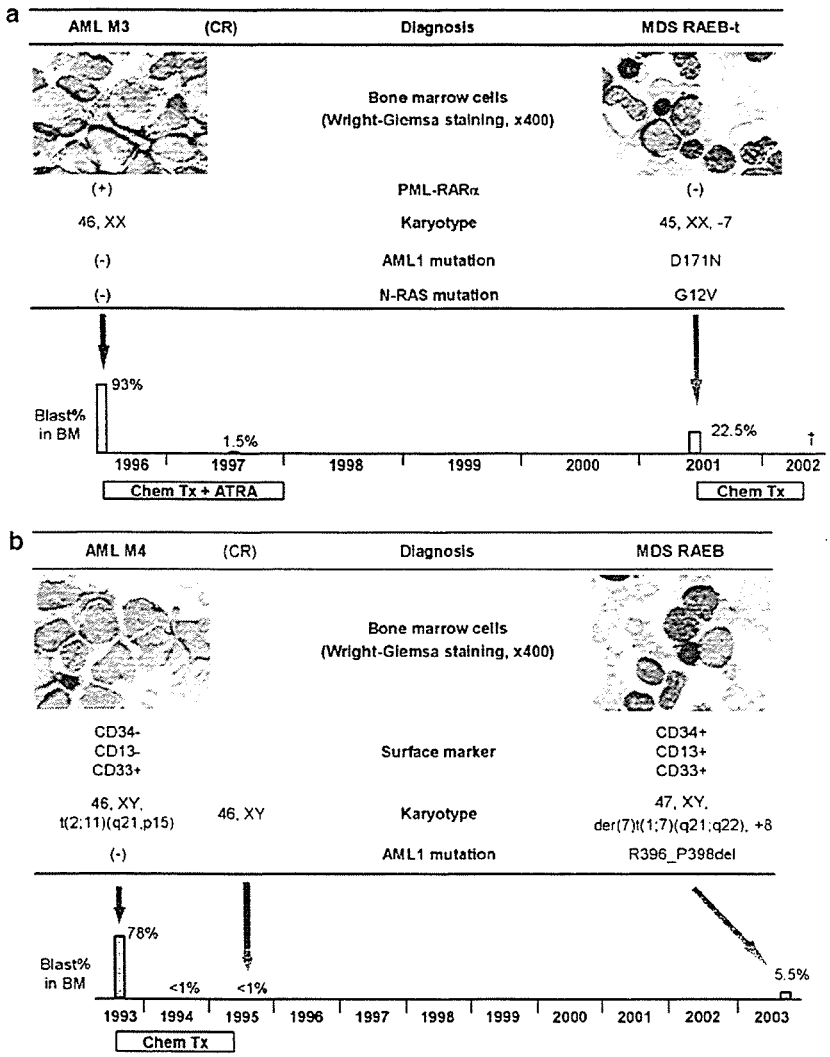

Figure 1 Clinical course of the patients developing MDS after chemotherapy for AML. (**a**) Case 8 was a female diagnosed as AML (M3) at the age of 38. She was treated with enocitabine, daunorubicin, vincristine, 6-mercaptoputine, prednisolone, mitoxantrone, etoposide, cyclophosphamide, aclalubichin, methotrexate and all-*trans* retinoic acid for a year and a half, leading to CCR. She developed MDS (RAEBt) at the age of 43. (**b**) Case 42 was a male diagnosed as AML (M4) at the age of 62. He was treated with enocitabine, daunorubicin, vincristine, 6-mercaptoputine, prednisolone, mitoxantrone, etoposide, cyclophosphamide, aclalubichin and methotrexate for two years, leading to CCR. He developed MDS (RAEB) at the age of 72. CR indicates complete remission; Chem Tx, chemotherapy; ATRA, all-*trans* retinoic acid.

Table 3 Frequency of genetic abnormalities in patients with MDS/AML or CBF leukemia

Genes	*MDS/AML patients*		P*	*CBF leukemia patients (N = 25)*
	With AML1 mutation (N = 34)	Without AML1 mutation (N = 80)		
N-RAS	5	3	0.0501	1
K-RAS	0	0	1	0
PTPN11	4	0	0.0069	0
NF1	2	0	0.0871	0
FLT3	4	2	0.0638	2
c-KIT	0	0	1	6
RTK–RAS pathway	13 (38%)	5 (6.3%)	<0.0001	9 (36%)
p53	0	12 (15%)	0.0170	0

RTK = receptor tyrosine kinase. *Fisher's exact probability test was used to determine the *P*-value.
N-RAS mutations were G12V, G13D, G60E, Q61K and Q61H; *PTPN11* mutations were N58Y, F71L and A72T; *NF1* mutations were C118fsX164 and S382fsX390; *FLT3* mutations were tandem duplications ranged in size from 7 to 24 amino acids and D835Y; *c-KIT* mutations were TYD417_419FG, D816A, D816Y and D816V; and *p53* mutations were Y126C, S127C, V143M, R175H, H179Y, H214R, Y234C, R248Q, Y236X and C275F.

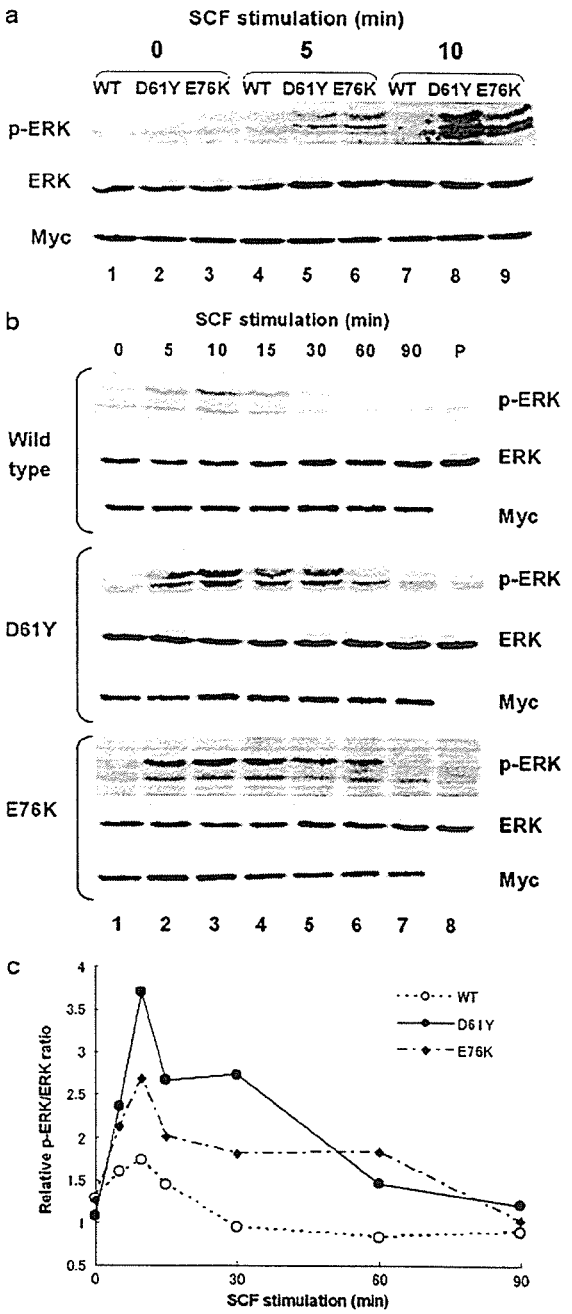

Figure 2 Effects of wild-type and mutant SHP-2 proteins on ERK activation in response to SCF. (a) HEL cells were transfected with an expression vector containing either wild-type SHP-2 or a mutated SHP-2 construct and stimulated with SCF (100 ng/ml) for 0, 5 or 10 min. The equivalent expression levels of wild-type, D61Y or E76K SHP-2 protein in total cell lysates were detected by immunoblot analysis with an anti-Myc antibody (Myc). Cell lysates were immunoblotted with an anti-p-ERK specific antibody to monitor ERK activation, or with an anti-ERK antibody (ERK) to confirm equivalent levels of ERK expression. (b) SHP2-overexpressed HEL cells were stimulated with SCF for up to 90 min. Parental HEL cells (labeled P) were also analyzed as a control. (c) The relative p-ERK/ERK ratio compared with parental HEL cells is presented.

abnormalities or by the patient's previous exposure to chemotherapy. Two main cytogenetic pathways have been proposed to explain the malignant transformation step in patients with therapy-related MDS (t-MDS):[29–31] pathway I is '−7/7q- with normal chromosome 5', and pathway II is '−5/5q-'. The patients belonging to the pathway I group frequently show mutations of *RAS* genes[32] and methylation of the $p15^{INK4b}$ gene promoter.[33] A more recent study has shown that *AML1* mutations in patients with t-MDS were highly significantly associated with −7/7q-.[5] On the other hand, patients belonging to pathway II frequently present a complex karyotype and a mutation of *p53*, whereas pathway I has a very low frequency of *p53* mutations.[22,34] However, we have focused on the pivotal role of AML1 mutations, rather than cytogenetic abnormalities, during the development of MDS/AML. We are trying to define the disease entity of 'MDS/AML with AML1 mutation', which could be considered for inclusion in the recurrent genetic abnormalities under the WHO classification. Thus, we have attempted to classify the genetic pathway of developing MDS/AML with or without AML1 mutations.

Many reports have shown that genes involved in the RAS signaling pathway are mutated in hematopoietic diseases. In MDS, mutations of the *N-RAS* gene have been known to be a frequent (~10%) genetic alteration,[35] and these typically occur during transformation to AML. However, mutations of *PTPN11* have been reported to be rare in adult MDS (2 of 189 MDS/AML, 1.1%),[36–38] although they have been frequently found in childhood MDS.[25] Mutations of the *NF1* gene are also very rare in adult MDS.[39] Mutations of the *FLT3* gene are found in 5% of MDS patients, and are associated with leukemic transformation.[40,41] In this study, we found a significantly higher mutation frequency of these genes in MDS/AML patients with AML1 mutations than in those without an AML1 mutation (38 versus 6.3%, $P<0.0001$). The high frequency of these mutations in patients with AML1 mutations leads us to consider that mutations in the RAS pathway, besides being valuable deciding factors for prognosis, may function also as genetic partners of the AML1 mutations. Mutations of *RAS*, *NF1* or *PTPN11* are seen in most patients with JMML, a MPD of young children.[28] All mouse models bearing a heterozygous *Nf1* ($Nf1^{+/-}$),[42] a conditional inactivation of *Nf1* ($Nf1^{-/-}$),[43] a conditional expression of activating *K-ras* mutation ($K\text{-}ras^{G12D/+}$),[44,45] or a heterozygous *Ptpn11* mutation ($Ptpn11^{D61G/+}$)[46] developed a myeloproliferative disease. Thus, we suggest that these gene alterations might work as 'proliferative' partners of the AML1 mutations.

Which ligand/receptor system would be involved in stimulation of this pathway? Most previous studies of gene mutations affecting the RAS pathway have revealed the hypersensitive proliferation of hematopoietic progenitor cells by using a stimulating ligand of GM-CSF, especially in the studies of JMML.[44,46,47] However, GM-CSF seems not to be essential for proliferation of hematopoietic stem cells expressing CD34 in patients with MDS. CD34-positive hematopoietic stem cells express the c-KIT receptor protein, and AML1 is required for the generation of these cells.[48] Moreover, c-KIT mutations and/or overexpression are frequently seen in patients with CBF leukemia in which AML1 functions are impaired (Table 3).[11,49,50] These gain-of-function mutations of c-KIT result not only in constitutive activation but also in receptor hyperactivation in response to SCF stimulation.[51] In the patients with AML1-mutated MDS/AML, a disease characterized by impaired AML1 function that is similar to CBF leukemia, we did not find any c-KIT mutation. However, blast cells of these patients expressed c-KIT, and SCF stimulation of c-KIT expressing HEL cells bearing SHP-2 mutants yielded hyperactivation of the RAS pathway (Figure 2). Taken together, these results suggest that SCF stimulation via the c-KIT receptor might be important

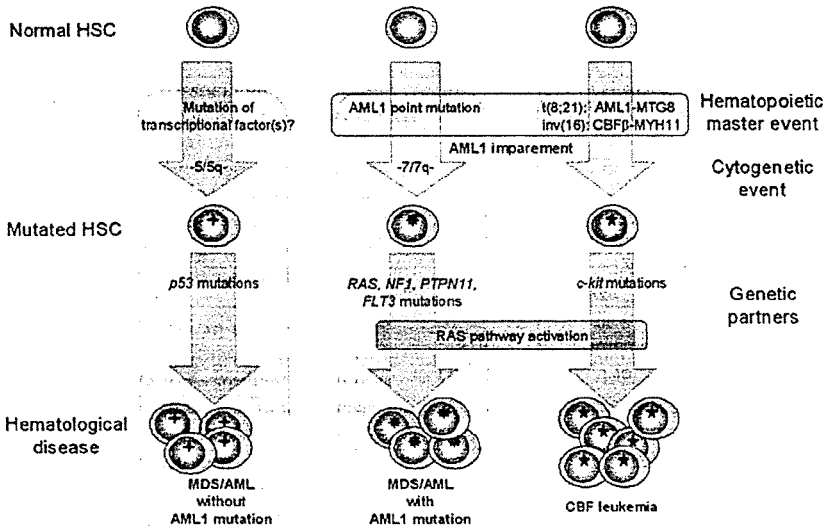

Figure 3 Genetic pathways in MDS/AML and in CBF leukemia.

for activating the RAS pathway in AML1-mutated MDS/AML patients, and hyperactivation of the RTK– (especially c-KIT–) RAS pathway may be a common genetic event in hematological malignancies with impaired AML1. In further support of this hypothesis, the AML1–ETO chimeric protein represses *NF1* expression.[52] The somatic mutations associated with some additional factors in the RTK–RAS pathway still remain unknown. Genes encoding these factors also might be altered in hematological diseases characterized by AML1 impairment. To clarify the cooperative functions of AML1 mutations and hyperactivation of the RAS pathway in development of MDS/AML, mice carrying both gene mutations are currently being established in our laboratory, and we will address these questions in future studies.

Here, we propose two genetic pathways in the development of MDS/AML (Figure 3). One is a pathway 'with AML1 mutation'. In this pathway, AML1 mutations, similar to chimeras in *de novo* AML, would be considered to be the major decision factor to develop MDS/AML and would inhibit the differentiation of hematopoietic stem cells. A hematopoietic stem cell that has acquired *AML1* gene mutation apparently requires a long latency period to be transformed and to be conferred a proliferative and/or survival advantage by gene alterations belonging to the RTK–RAS signal transduction pathways, leading to development of MDS/AML. During this process, loss of the long arm of chromosome 7, the critical region at 7q22.1 possibly related to DNA repair genes,[53] would also play an important role in this pathway. It is suspected that some more patients with MDS/AML who have an AML1 haploinsufficiency so far undetected (such as micro-deletion of 21q22, methylation of the promoter, etc.) still exist, and they should be included in this pathway. The other pathway is one without an AML1 mutation. In this pathway, the master genetic events that inhibit the differentiation of hematopoietic stem cells are still unknown. However, patients without AML1 mutation frequently show the 5q- chromosomal abnormality. A recent paper showed that mice carrying heterozygous *Nucleophosmin 1* gene, which maps to 5q35 in human, developed a hematological syndrome with features of human MDS.[54] Haploinsufficiency of nucleophosmin might be one of the master genetic events of the pathogenesis of MDS/AML in this pathway. Furthermore, *p53* gene alterations are considered to work as a genetic partner leading to development of MDS/AML in this pathway. Identification of a relevant genetic pathway in MDS/AML pathogenesis may lead us to develop new therapies based on a clearer understanding of disease biology.

Acknowledgements

This work was supported in part by Grants-in-Aid for Scientific Research from the Ministry of Education, Culture, Sports, Science and Technology of Japan, the Osaka Cancer Research Foundation, and the Tsuchiya Foundation. We are grateful to Ryoko Matsumoto-Yamaguchi for excellent technical support in carrying out these experiments. We also thank Dr Ross Fisher and Dr Hideaki Nakajima for critical reading of the article.

References

1 Osato M, Asou N, Abdalla E, Hoshino K, Yamasaki H, Okubo T *et al.* Biallelic and heterozygous point mutations in the runt domain of the AML1/PEBP2alphaB gene associated with myeloblastic leukemias. *Blood* 1999; **93**: 1817–1824.
2 Preudhomme C, Warot-Loze D, Roumier C, Grardel-Duflos N, Garand R, Lai JL *et al.* High incidence of biallelic point mutations in the Runt domain of the AML1/PEBP2 alpha B gene in Mo acute myeloid leukemia and in myeloid malignancies with acquired trisomy 21. *Blood* 2000; **96**: 2862–2869.
3 Silva FP, Morolli B, Storlazzi CT, Anelli L, Wessels H, Bezrookove V *et al.* Identification of RUNX1/AML1 as a classical tumor suppressor gene. *Oncogene* 2003; **22**: 538–547.
4 Harada H, Harada Y, Tanaka H, Kimura A, Inaba T. Implications of somatic mutations in the AML1 gene in radiation-associated and therapy-related myelodysplastic syndrome/acute myeloid leukemia. *Blood* 2003; **101**: 673–680.
5 Christiansen DH, Andersen MK, Pedersen-Bjergaard J. Mutations of AML1 are common in therapy-related myelodysplasia following therapy with alkylating agents and are significantly associated with deletion or loss of chromosome arm 7q and with subsequent leukemic transformation. *Blood* 2004; **104**: 1474–1481.
6 Song WJ, Sullivan MG, Legare RD, Hutchings S, Tan X, Kufrin D *et al.* Haploinsufficiency of CBFA2 causes familial thrombocytopenia

with propensity to develop acute myelogenous leukaemia. *Nat Genet* 1999; **23**: 166–175.
7 Osato M. Point mutations in the RUNX1/AML1 gene: another actor in RUNX leukemia. *Oncogene* 2004; **23**: 4284–4296.
8 Harada H, Harada Y, Niimi H, Kyo T, Kimura A, Inaba T. High incidence of somatic mutations in the AML1/RUNX1 gene in myelodysplastic syndrome and low blast percentage myeloid leukemia with myelodysplasia. *Blood* 2004; **103**: 2316–2324.
9 Ichikawa M, Asai T, Saito T, Yamamoto G, Seo S, Yamazaki I *et al.* AML-1 is required for megakaryocytic maturation and lymphocytic differentiation, but not for maintenance of hematopoietic stem cells in adult hematopoiesis. *Nat Med* 2004; **10**: 299–304.
10 Higuchi M, O'Brien D, Kumaravelu P, Lenny N, Yeoh EJ, Downing JR. Expression of a conditional AML1-ETO oncogene bypasses embryonic lethality and establishes a murine model of human t(8;21) acute myeloid leukemia. *Cancer Cell* 2002; **1**: 63–74.
11 Beghini A, Peterlongo P, Ripamonti CB, Larizza L, Cairoli R, Morra E *et al.* C-kit mutations in core binding factor leukemias. *Blood* 2000; **95**: 726–727.
12 Gilliland DG. Hematologic malignancies. *Curr Opin Hematol* 2001; **8**: 189–191.
13 Matsuno N, Osato M, Yamashita N, Yanagida M, Nanri T, Fukushima T *et al.* Dual mutations in the AML1 and FLT3 genes are associated with leukemogenesis in acute myeloblastic leukemia of the M0 subtype. *Leukemia* 2003; **17**: 2492–2499.
14 Fenaux P. Chromosome and molecular abnormalities in myelodysplastic syndromes. *Int J Hematol* 2001; **73**: 429–437.
15 Hirai H. Molecular mechanisms of myelodysplastic syndrome. *Jpn J Clin Oncol* 2003; **33**: 153–160.
16 Rosenfeld C, List A. A hypothesis for the pathogenesis of myelodysplastic syndromes: implications for new therapies. *Leukemia* 2000; **14**: 2–8.
17 Mitelman F (ed). *An International System for Human Cytogenetic Nomenclature (1995): Recommendations of the International Standing Committee on Human Cytogenetic Nomenclature.* Basel, Switzerland: S Karger,, 1995.
18 Bowen DT, Frew ME, Rollinson S, Roddam PL, Dring A, Smith MT *et al.* CYP1A1*2B (Val) allele is overrepresented in a subgroup of acute myeloid leukemia patients with poor-risk karyotype associated with NRAS mutation, but not associated with FLT3 internal tandem duplication. *Blood* 2003; **101**: 2770–2774.
19 Pullarkat VA, Bueso-Ramos C, Lai R, Kroft S, Wilson CS, Pullarkat ST *et al.* Systemic mastocytosis with associated clonal hematological non-mast-cell lineage disease: analysis of clinicopathologic features and activating c-kit mutations. *Am J Hematol* 2003; **73**: 12–17.
20 Tartaglia M, Kalidas K, Shaw A, Song X, Musat DL, van der Burgt I *et al.* PTPN11 mutations in Noonan syndrome: molecular spectrum, genotype-phenotype correlation, and phenotypic heterogeneity. *Am J Hum Genet* 2002; **70**: 1555–1563.
21 De Luca A, Buccino A, Gianni D, Mangino M, Giustini S, Richetta A *et al.* NF1 gene analysis based on DHPLC. *Hum Mutat* 2003; **21**: 171–172.
22 Christiansen DH, Andersen MK, Pedersen-Bjergaard J. Mutations with loss of heterozygosity of p53 are common in therapy-related myelodysplasia and acute myeloid leukemia after exposure to alkylating agents and significantly associated with deletion or loss of 5q, a complex karyotype, and a poor prognosis. *J Clin Oncol* 2001; **19**: 1405–1413.
23 Kiyoi H, Naoe T, Nakano Y, Yokota S, Minami S, Miyawaki S *et al.* Prognostic implication of FLT3 and N-RAS gene mutations in acute myeloid leukemia. *Blood* 1999; **93**: 3074–3080.
24 Yamamoto Y, Kiyoi H, Nakano Y, Suzuki R, Kodera Y, Miyawaki S *et al.* Activating mutation of D835 within the activation loop of FLT3 in human hematologic malignancies. *Blood* 2001; **97**: 2434–2439.
25 Tartaglia M, Niemeyer CM, Fragale A, Song X, Buechner J, Jung A *et al.* Somatic mutations in PTPN11 in juvenile myelomonocytic leukemia, myelodysplastic syndromes and acute myeloid leukemia. *Nat Genet* 2003; **34**: 148–150.
26 Fragale A, Tartaglia M, Wu J, Gelb BD. Noonan syndrome-associated SHP2/PTPN11 mutants cause EGF-dependent prolonged GAB1 binding and sustained ERK2/MAPK1 activation. *Hum Mutat* 2004; **23**: 267–277.
27 Chan RJ, Leedy MB, Munugalavadla V, Voorhorst CS, Li Y, Yu M *et al.* Human somatic PTPN11 mutations induce hematopoietic cell hypersensitivity to granulocyte-macrophage colony stimulating factor. *Blood* 2005; **105**: 3737–3742.
28 Loh ML, Vattikuti S, Schubbert S, Reynolds MG, Carlson E, Lieuw KH *et al.* Mutations in PTPN11 implicate the SHP-2 phosphatase in leukemogenesis. *Blood* 2004; **103**: 2325–2331.
29 Pedersen-Bjergaard J, Andersen MK, Christiansen DH, Nerlov C. Genetic pathways in therapy-related myelodysplasia and acute myeloid leukemia. *Blood* 2002; **99**: 1909–1912.
30 Pedersen-Bjergaard J, Christiansen DH, Andersen MK, Skovby F. Causality of myelodysplasia and acute myeloid leukemia and their genetic abnormalities. *Leukemia* 2002; **16**: 2177–2184.
31 Qian Z, Fernald AA, Godley LA, Larson RA, Le Beau MM. Expression profiling of CD34+ hematopoietic stem/progenitor cells reveals distinct subtypes of therapy-related acute myeloid leukemia. *Proc Natl Acad Sci USA* 2002; **99**: 14925–14930.
32 Stephenson J, Lizhen H, Mufti GJ. Possible co-existence of RAS activation and monosomy 7 in the leukaemic transformation of myelodysplastic syndromes. *Leuk Res* 1995; **19**: 741–748.
33 Christiansen DH, Andersen MK, Pedersen-Bjergaard J. Methylation of p15INK4B is common, is associated with deletion of genes on chromosome arm 7q and predicts a poor prognosis in therapy-related myelodysplasia and acute myeloid leukemia. *Leukemia* 2003; **17**: 1813–1819.
34 Horiike S, Misawa S, Kaneko H, Sasai Y, Kobayashi M, Fujii H *et al.* Distinct genetic involvement of the TP53 gene in therapy-related leukemia and myelodysplasia with chromosomal losses of Nos 5 and/or 7 and its possible relationship to replication error phenotype. *Leukemia* 1999; **13**: 1235–1242.
35 Hirai H, Kobayashi Y, Mano H, Hagiwara K, Maru Y, Omine M *et al.* A point mutation at codon 13 of the N-ras oncogene in myelodysplastic syndrome. *Nature* 1987; **327**: 430–432.
36 Johan MF, Bowen DT, Frew ME, Goodeve AC, Wilson GA, Peake IR *et al.* Mutations in PTPN11 are uncommon in adult myelodysplastic syndromes and acute myeloid leukaemia. *Br J Haematol* 2004; **124**: 843–844.
37 Watkins F, Fidler C, Boultwood J, Wainscoat JS. Mutations in PTPN11 are rare in adult myelodysplastic syndromes and acute myeloid leukemia. *Am J Hematol* 2004; **76**: 417.
38 Loh ML, Martinelli S, Cordeddu V, Reynolds MG, Vattikuti S, Lee CM *et al.* Acquired PTPN11 mutations occur rarely in adult patients with myelodysplastic syndromes and chronic myelomonocytic leukemia. *Leuk Res* 2005; **29**: 459–462.
39 Kaneko H, Horiike S, Nakai H, Ueda Y, Nakao M, Hirakawa K *et al.* Neurofibromatosis 1 gene (NF1) mutation is a rare genetic event in myelodysplastic syndrome regardless of the disease progression. *Int J Hematol* 1995; **61**: 113–116.
40 Yokota S, Kiyoi H, Nakao M, Iwai T, Misawa S, Okuda T *et al.* Internal tandem duplication of the FLT3 gene is preferentially seen in acute myeloid leukemia and myelodysplastic syndrome among various hematological malignancies. A study on a large series of patients and cell lines. *Leukemia* 1997; **11**: 1605–1609.
41 Horiike S, Yokota S, Nakao M, Iwai T, Sasai Y, Kaneko H *et al.* Tandem duplications of the FLT3 receptor gene are associated with leukemic transformation of myelodysplasia. *Leukemia* 1997; **11**: 1442–1446.
42 Jacks T, Shih TS, Schmitt EM, Bronson RT, Bernards A, Weinberg RA. Tumour predisposition in mice heterozygous for a targeted mutation in Nf1. *Nat Genet* 1994; **7**: 353–361.
43 Le DT, Kong N, Zhu Y, Lauchle JO, Aiyigari A, Braun BS *et al.* Somatic inactivation of Nf1 in hematopoietic cells results in a progressive myeloproliferative disorder. *Blood* 2004; **103**: 4243–4250.
44 Braun BS, Tuveson DA, Kong N, Le DT, Kogan SC, Rozmus J *et al.* Somatic activation of oncogenic Kras in hematopoietic cells initiates a rapidly fatal myeloproliferative disorder. *Proc Natl Acad Sci USA* 2004; **101**: 597–602.
45 Chan IT, Kutok JL, Williams IR, Cohen S, Kelly L, Shigematsu H *et al.* Conditional expression of oncogenic K-ras from its endogenous promoter induces a myeloproliferative disease. *J Clin Invest* 2004; **113**: 528–538.
46 Araki T, Mohi MG, Ismat FA, Bronson RT, Williams IR, Kutok JL *et al.* Mouse model of Noonan syndrome reveals cell type- and

gene dosage-dependent effects of Ptpn11 mutation. *Nat Med* 2004; **10**: 849–857.
47 Donovan S, See W, Bonifas J, Stokoe D, Shannon KM. Hyperactivation of protein kinase B and ERK have discrete effects on survival, proliferation, and cytokine expression in Nf1-deficient myeloid cells. *Cancer Cell* 2002; **2**: 507–514.
48 Yokomizo T, Ogawa M, Osato M, Kanno T, Yoshida H, Fujimoto T *et al*. Requirement of Runx1/AML1/PEBP2alphaB for the generation of haematopoietic cells from endothelial cells. *Genes Cells* 2001; **6**: 13–23.
49 Care RS, Valk PJ, Goodeve AC, Abu-Duhier FM, Geertsma-Kleinekoort WM, Wilson GA *et al*. Incidence and prognosis of c-KIT and FLT3 mutations in core binding factor (CBF) acute myeloid leukaemias. *Br J Haematol* 2003; **121**: 775–777.
50 Wang YY, Zhou GB, Yin T, Chen B, Shi JY, Liang WX *et al*. AML1-ETO and C-KIT mutation/overexpression in t(8;21) leukemia: implication in stepwise leukemogenesis and response to Gleevec. *Proc Natl Acad Sci USA* 2005; **102**: 1104–1109.
51 Kohl TM, Schnittger S, Ellwart JW, Hiddemann W, Spiekermann K. KIT exon 8 mutations associated with core binding factor (CBF) – acute myeloid leukemia (AML) cause hyperactivation of the receptor in response to stem cell factor. *Blood* 2004; **105**: 3319–3321.
52 Yang G, Khalaf W, van de Locht L, Jansen JH, Gao M, Thompson MA *et al*. Transcriptional Repression of the neurofibromatosis-1 tumor suppressor by the t(8;21) fusion protein. *Mol Cell Biol* 2005; **25**: 5869–5879.
53 Johnson EJ, Scherer SW, Osborne L, Tsui LC, Oscier D, Mould S *et al*. Molecular definition of a narrow interval at 7q22*1 associated with myelodysplasia. *Blood* 1996; **87**: 3579–3586.
54 Grisendi S, Bernardi R, Rossi M, Cheng K, Khandker L, Manova K *et al*. Role of nucleophosmin in embryonic development and tumorigenesis. *Nature* 2005; **437**: 147–153.

Supplementary Information accompanies the paper on the Leukemia website (http://www.nature.com/leu)

Molecular Cell
Article

Cytokines Direct the Regulation of Bim mRNA Stability by Heat-Shock Cognate Protein 70

Hirotaka Matsui,[1] Hiroya Asou,[1] and Toshiya Inaba[1,*]
[1] Department of Molecular Oncology and Leukemia Program Project, Research Institute for Radiation Biology and Medicine, Hiroshima University, Hiroshima 734-8553, Japan
*Correspondence: tinaba@hiroshima-u.ac.jp
DOI 10.1016/j.molcel.2006.12.007

SUMMARY

Previous gene-targeting studies indicated that Bim, a BH3-only death activator, regulates total blood cell number. Cytokines contribute to this process by negatively regulating steady-state levels of Bim mRNA. Here we present a molecular mechanism for cytokine-mediated posttranscriptional regulation of Bim mRNA by heat-shock cognate protein 70 (Hsc70), which binds to AU-rich elements (AREs) in the 3′-untranslated region of specific mRNAs and enhances their stability. The RNA binding potential of Hsc70 is regulated by cochaperones including Bag-4 (also SODD), CHIP, Hip, and Hsp40. Cytokines regulate the expression or function of these cochaperones by activating Ras pathways. Thus, exposure of cells to cytokines ultimately leads to destabilization of Bim mRNA and promotion of cell survival. This unanticipated role of a chaperone/cochaperone complex in mRNA stability appears to be critical for hematopoiesis and leukemogenesis.

INTRODUCTION

Cytokines promote cell survival of hematopoietic progenitors by negative regulation of Bim (O'Connor et al., 1998; Hsu et al., 1998), a BH3-only cell death activator in the Bcl-2 superfamily (reviewed in Inaba [2004]). Neurotrophic factors promote the survival of neuronal cells, also by negative regulation of Bim (reviewed in Freeman et al. [2004]). Bim-deficient mice, which manifest both hyperplasia of hematopoietic progenitors and increased white blood cell count (Bouillet et al., 1999), support Bim's role in hematopoiesis. In addition, T cell development is perturbed, and older knockout mice accumulate plasma cells and succumb to autoimmune kidney disease. Cytokines also control the activity of $p27^{KIP1}$ (Toyoshima and Hunter, 1994). Disruption of the murine p27 gene results in hyperplasia of all organs, including hematopoietic progenitors in the spleen and T cells in the thymus (Fero et al., 1996). Thus, cytokine regulation of Bim and p27 is critical for cell-number homeostasis, especially in the hematopoietic and immune systems.

The molecular mechanisms by which cytokines negatively regulate Bim function differ between cell types. At least three different mechanisms have been reported (reviewed in Inaba [2004]). First, steady-state levels of Bim mRNA decrease in the murine hematopoietic progenitor cell lines Baf-3 and FL5.12 in response to IL-3-mediated activation of Ras pathways (Shinjyo et al., 2001; Dijkers et al., 2000a). Nerve growth factor (NGF) functions similarly as a negative regulator of Bim in primary cultures of rat sympathetic neurons and PC-12 cells (reviewed in Freeman et al. [2004]). Second, serum- or cytokine-dependent phosphorylation of Bim enhances its ubiquitination, which is known to regulate the proteasome-dependent degradation of Bim in serum-deprived fibroblasts and M-CSF-dependent osteoclasts (Ley et al., 2003; Akiyama et al., 2003; Luciano et al., 2003). Third, IL-3 affects the subcellular localization of Bim in murine FDC-P1 cells (Puthalakath et al., 1999), in which IL-3 promotes Bim binding to dynein motor complexes on microtubules. Upon withdrawal of IL-3, Bim dissociates from microtubules and then binds to and inhibits antiapoptotic Bcl-2 protein function.

The diversity of these regulatory mechanisms suggests that regulation of Bim function is multifaceted, allowing flexibility in Bim's response to different signals or in different cell types (Yamaguchi et al., 2003). Observations in our laboratory demonstrate that hematopoietic homeostasis is sensitive to changes in steady-state Bim mRNA levels, in that Bim mRNA levels increase in bone marrow-derived $Sca\text{-}1^{+}c\text{-}Kit^{+}Lin^{-}$ cells that are deprived of stem cell factor (SCF) and thrombopoietin (TPO) (Kuribara et al., 2004). In addition, recent studies indicate that cytokines also regulate steady-state levels of p27 mRNA (Dijkers et al., 2000b; Parada et al., 2001; Stahl et al., 2002), although, prior to these reports, regulation of p27 activity was thought to occur predominantly via cyclin E-cdk2-mediated phosphorylation, which targets p27 for proteasome-dependent degradation. These results suggest that cytokine deprivation can decrease cell number in the body by promoting increases in Bim and p27 mRNA levels.

NGF-mediated regulation of Bim in PC12 cells depends on sequence-specific DNA binding sites for FOXO3a (also

FKHR-L1), located in the Bim enhancer (Gilley et al., 2003). p27 gene transcription in Baf-3 cells has also been reported to be regulated by FOXO3a (Dijkers et al., 2000b). Since FOXO3a is inactivated by Ras-mediated phosphorylation events (reviewed in Birkenkamp and Coffer [2003]), we initially hypothesized that FOXO3a regulated the cytokine-dependent transcription of Bim in hematopoietic cells. However, experiments in Baf-3 cells demonstrated no IL-3-dependent *cis*-acting regulatory elements in Bim (Matsui et al., 2005). Furthermore, FOXO3a binding sites within Bim (which function as NGF-dependent enhancers in PC12 cells) did not affect Bim transcription efficiency in Baf-3 cells, and de novo transcription of Bim in Baf-3 cells was similar in the presence or absence of IL-3. These data led to the alternative hypothesis that IL-3-dependent decreases in Bim mRNA levels occur posttranscriptionally.

Here, we report that cytokines regulate Bim mRNA stability in Baf-3 cells. Binding of heat-shock cognate protein 70 (Hsc70), which stabilizes Bim mRNA, is regulated by the cytokine-dependent association of cochaperones with Hsc70. We suggest that this mechanism plays a critical role in the regulation of hematopoietic cell number in the body.

RESULTS

Destabilization of Bim mRNA by IL-3 in Baf-3 Cells

The 3′UTR of human Bim mRNA is long (4.2 kb) relative to the coding region (0.6 kb) (Figure 1A). The 3′UTR contains a number of AUUUA pentamer repeats, which are *cis*-acting sequences within AU-rich sequence elements (AREs) that are critical to the regulation of mRNA stability. In a comparison between the eight pentamers in human mRNA and six in mouse mRNA, four are conserved. Although the overall sequence homology is low between human and mouse Bim 3′UTRs, there is 76% conservation within a 1 kb region that includes three AUUUA pentamers.

To assess the role of the Bim 3′UTR on mRNA stability, IL-3-dependent Baf-3 cells were transfected with Tet-regulated plasmids expressing full-length β-globin mRNA (control) or an mRNA hybrid of β-globin coding sequence terminated by the Bim 3′UTR. Expression was induced for 3 hr and then shut off. mRNA decay was measured by using ribonuclease protection assay (RPA) and real-time quantitative RT-PCR (qRT-PCR). As previously demonstrated (Xu et al., 1998), full-length β-globin mRNA expressed in Baf-3 cells was stable in the presence or absence of IL-3 (Figures 1B and 1C). In contrast, the stability of the β-globin/Bim hybrid mRNA was reduced significantly in the presence of IL-3.

The half-lives of Bim, p27, and c-*fos* mRNAs synthesized and radiolabeled in vitro were measured in Baf-3-cell cytosol (S100) extracts. The half-life of a 1 kb Bim mRNA encompassing the conserved region between human and mouse 3′UTRs was less than 10 min in extracts from IL-3-treated Baf-3 cells (Figures 1D and 1E) but increased significantly to ~30 min in extracts prepared from cells without IL-3. The half-life of p27 3′UTR mRNA increased similarly in IL-3-starved cell extracts. IL-3-dependent message destabilization in Baf-3 extracts was not universal, since the half-lives of c-*fos* mRNA (<10 min) and GAPDH mRNA (>30 min) remained constant in the presence or absence of IL-3. Moreover, the 30 min half-life of Bim mRNA in lysates from FDC-P1 cells (another IL-3-dependent cell line in which Bim expression is not affected by IL-3) did not vary in the presence or absence of IL-3.

mRNA decay generally initiates with poly(A) tail deadenylation followed by degradation of internal sequences. To observe shortening of the poly(A) tail, we repeated the in vitro RNA decay assay using short mRNAs (~60 bases) containing native AREs and a 100 base poly(A) tail. With or without IL-3, deadenylation of GAPDH control mRNA was detected at 20 min, similar to Bim and p27 mRNAs in cytosol preparations from IL-3-starved Baf-3 cells (Figure 1F). In contrast, deadenylation of Bim and p27 mRNAs initiated within 5 min and progressed rapidly in extracts from IL-3 treated Baf-3 cells. When 5′-capped Bim mRNA without a poly(A) tail was mixed with Baf-3 cell extracts, both the 1 kb conserved region and the short ARE in the 3′ UTR degraded more rapidly in the presence of IL-3 (Figure 1G). These data demonstrate that IL-3 destabilization of mRNAs in Baf-3 cells is gene and cell type specific and occurs by stimulation of mRNA deadenylation and degradation.

Hsc70 Binds to Bim mRNA in an IL-3-Dependent Manner

To identify RNA binding proteins that may function as IL-3-dependent stabilizing or destabilizing factors, RNA-affinity chromatography was used to enrich for cytosolic proteins that bind to Bim's 3′UTR. When cytosolic extracts of Baf-3 or FL5.12 cells were exposed to columns coupled with the 3′UTR of Bim or p27 mRNA, the bound fractions resolved with similar patterns in SDS-polyacrylamide gels (Figure 2A). In particular, the intensity of one band (~75 kDa) was greater in IL-3-starved Baf-3 or FL5.12 cells relative to cells cultured with IL-3. In contrast, the signal from the 75 kDa band was weak and did not vary in the presence or absence of IL-3 when eluted from GAPDH (containing no ARE) or c-*fos* 3′UTR mRNA columns. The pattern of FDC-P1 extract proteins bound to Bim mRNA showed significantly less 75 kDa signal.

Polypeptide bands at the position of 75 kDa were excised from the gel and analyzed by using a MALDI-TOF/TOF mass spectrometer. In peptide mass fingerprinting, the molecular weights of nine peaks matched mouse Hsc70 (Figure 2B), and mass spectrometric sequencing of these peaks also matched Hsc70 (Figure 2C). Proteins bound to the Bim 3′UTR column showed a 6-fold increase in reactivity to Hsc70-specific antibody when isolated from IL-3 starved Baf-3 cells relative to cells grown with IL-3 (Figure 2D), whereas the Hsc70 signal was weak in Bim 3′UTR binding proteins from FDC-P1 cells both in the presence and absence of IL-3. No Hsp70 (closely

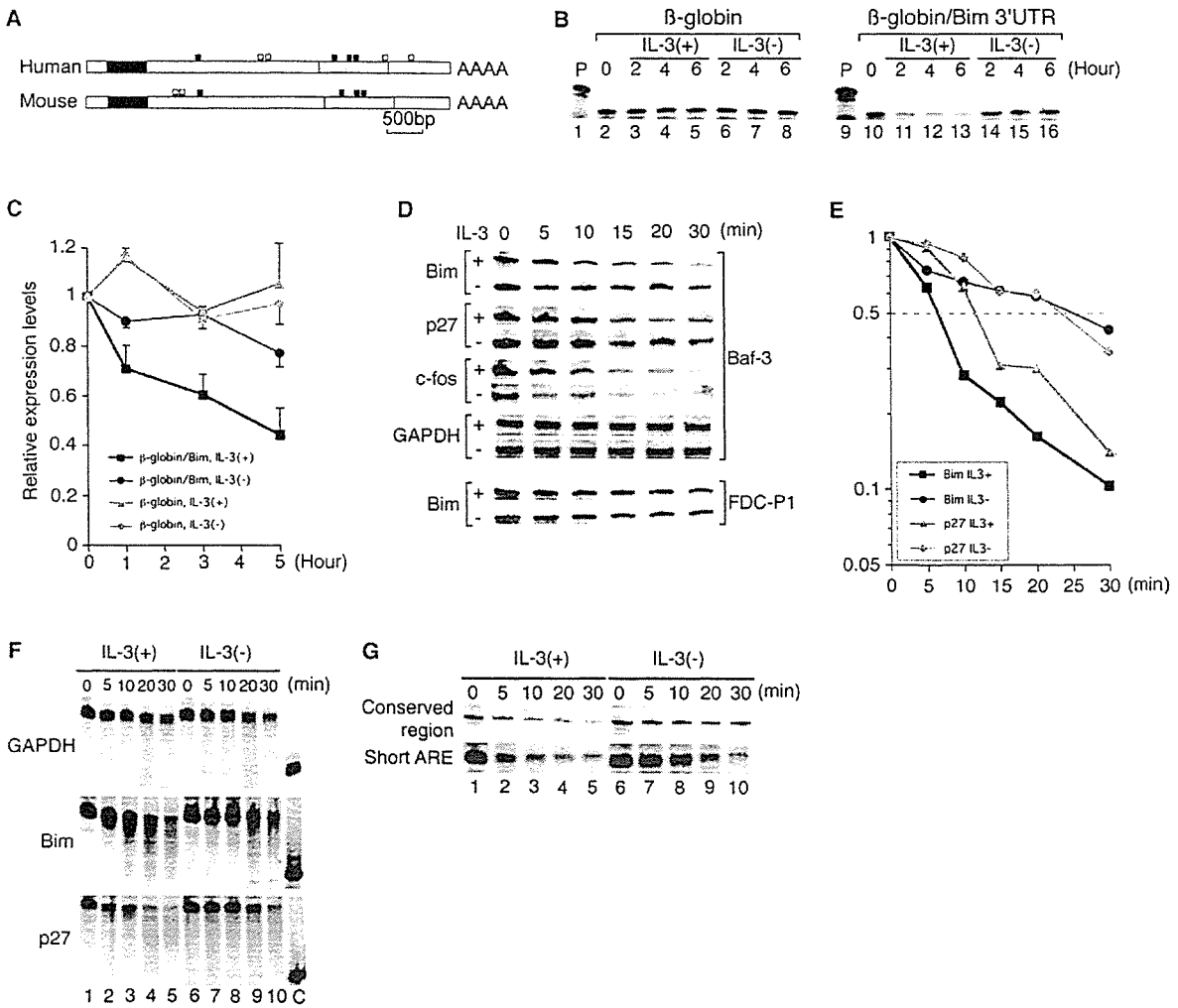

Figure 1. Stability of Bim mRNA

(A) A schematic representation of human and mouse Bim mRNAs. Black bars represent the coding regions, open bars untranslated regions, and gray bars regions of strong homology between human and mouse. Black squares above bars indicate AUUUA pentamers conserved between the human and mouse 3'UTRs; open squares are those present in either human or mouse.

(B and C) Stability of a β-globin/Bim 3'UTR fusion mRNA and β-globin mRNA (control) transiently expressed in Baf-3 cells cultured in the presence or absence of IL-3 and measured using RPA (B) or qRT-PCR (C). The mean and SD of three independent experiments are shown.

(D–G) RNA-stability assays in vitro. Cytosol preparations from Baf-3 or FDC-P1 cells (D, indicated at right) cultured in the presence or absence of IL-3 were incubated for indicated periods with radiolabeled and capped mRNAs (genes marked at left) with (D–F) or without (G) a poly(A) tail of 100 residues. Values for each band were measured and plotted as percent relative to starting point levels (E).

related to Hsc70) was detected in the Bim 3'UTR-bound fraction of Baf-3 cells grown in the presence or absence of IL-3.

Hsc70 and Hsp70 have been shown to bind to AREs (Henics et al., 1999; Wilson et al., 2001; Duttagupta et al., 2003), and its binding is enhanced by Hsp40 (Zimmer et al., 2001). Binding of Hsc70 to Bim mRNA and the effect of recombinant Hsp40 (DjB1) protein was tested in vitro with a Bim 3'UTR probe containing two conserved AUUUA pentamers. Although the probe was not shifted above background in the presence of Hsc70 or Hsp40 alone, an equimolar mixture of Hsc70, Hsp40, and a co-chaperone, Hip (Hohfeld et al., 1995; we discuss later in detail) retarded the mobility of the RNA (Figure 2E). In the presence of Hsc70 or Hsp40 antibodies, the mobility of this complex was retarded further, suggesting that two proteins coassociate with Bim mRNA.

To test whether Hsc70 binds to RNA directly, mixtures of recombinant Hsc70, Hsp40, and Hip with radiolabeled AREs of Bim, GAPDH, or c-*fos* were UV crosslinked and resolved by SDS-PAGE. A single protein band of ~75 kDa was observed with a Bim mRNA probe, but not with GAPDH or c-*fos* probes (Figure 2F, lanes 1–3). In experiments using extracts from Baf-3 cells cultured with or

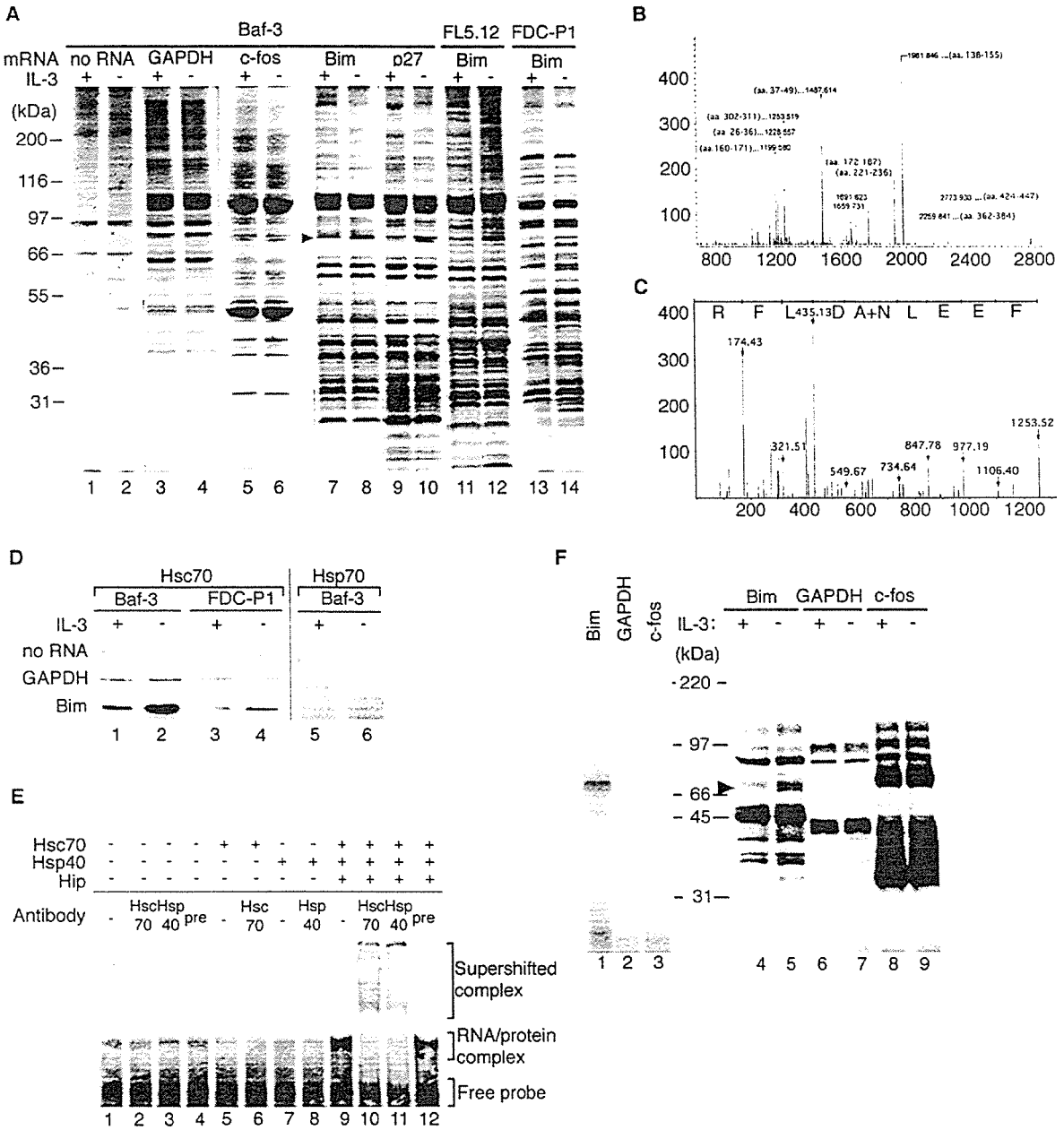

Figure 2. Hsc70 Binds to Bim mRNA

(A) RNA-affinity chromatography to enrich for proteins (in the cell types indicated above) that bind to the 3′UTRs of GAPDH, c-*fos*, Bim, or p27 mRNAs. Proteins were visualized by silver staining. An arrowhead indicates bands analyzed by MALDI-TOF/TOF.

(B) A representative result of peptide mass fingerprinting from MALDI-TOF analysis. The molecular weight of each peak and the corresponding amino acid residues of Hsc70 are shown.

(C) An example of protein sequencing using MALDI-TOF/TOF analysis. The MS/MS spectrum was recorded from the fragmentation of an ion at 1253.519. The interpretation of this spectrum gave the putative sequence FEEL(A+N)DLFR, where (A+N) denotes either AN or NA. This sequence matched aa 302–311 (FEELNADLFR) in mouse Hsc70.

(D) Hsc70- or Hsp70-specific antibody was used in immunoblots of fractions of Baf-3 and FDCP-1 cell extracts that bound to beads with no RNA, the 3′UTR of GAPDH or Bim mRNA.

(E) RNA gel retardation assay. A radiolabeled Bim mRNA probe was mixed with recombinant proteins as indicated above. Anti-Hsc70, anti-Hsp40, or preimmune serum was present as indicated.

(F) UV-crosslinking assay. Mixture of recombinant Hsc70, Hsp40, and Hip (lanes 1–3) or Baf-3 cell lysates cultured in the presence or absence of IL-3 (lanes 4–9) was incubated with radiolabeled Bim, GAPDH, or c-*fos* mRNA. An arrowhead indicates a band enhanced by IL-3 starvation.

without IL-3 (lanes 4–9), numerous protein bands were detected, including one at 75 kDa that was relatively more abundant in cells grown in the absence of IL-3 (arrowhead), while other crosslinked complexes were similar in intensity in cells grown with or without IL-3. When the same extracts were crosslinked with GAPDH or c-*fos* 3′UTR mRNAs, banding patterns differed substantially and showed little 75 kDa complex. These results indicated that Hsc70 interacts directly with Bim mRNA.

Hsc70 Stabilizes Bim mRNA

We established Baf-3 cells expressing Hsc70 at low levels using short hairpin RNA (shRNA)-expression plasmid vectors, piGENE-mU6-Hsc70#5 and #6, each of which targets a different sequence in Hsc70 mRNA. In two representative clones, #5-7 and #6-6 (Figure 3A), transiently expressed β-globin/Bim hybrid mRNA degraded rapidly in the presence or absence of IL-3, whereas steady-state levels of full-length β-globin mRNA were stable (Figure 3B). In in vitro mRNA decay assay, rapid deadenylation and degradation of Bim mRNA in extracts from clones #5-7 and #6-6 was observed regardless of IL-3 presence (Figure 3C).

IL-3 starvation increases steady-state levels of Bim mRNA in parent Baf-3 cells (Shinjyo et al., 2001) (Figure 3D and 3E). Consequently, upon removal of IL-3, steady-state levels of BimEL, BimL, and BimS proteins (encoded by alternatively spliced mRNAs) increase steadily (Figure 3F), and massive cell death initiates approximately 12 hr after IL-3 removal (Figure 3G). Relative to parent Baf-3 cells, IL-3 starvation weakly increased Bim mRNA levels in #5-7 and #6-6 cells (Figures 3D and 3E), yielding only marginal increases in Bim proteins (Figure 3F) and delaying apoptosis (Figure 3G). These data suggest that increases in the steady-state level of Bim mRNA are due primarily to mRNA stabilization and accumulation, which occur by Hsc70 stabilization of mRNAs in response to cytokine starvation.

Cochaperones Regulate the RNA Binding Potential of Hsc70

Since IL-3 starvation had no effect on the steady-state levels of Hsc70 protein in Baf-3 cells (Figure 4A), we hypothesized that IL-3 negatively regulates the RNA binding potential of Hsc70. As a test, we compared the binding of radiolabeled Bim 3′UTR mRNA to immunoprecipitated Hsc70 protein complexes isolated from Baf-3 cells cultured with or without IL-3. Hsc70 protein was recovered efficiently from IL-3-treated or -untreated cells by immunoprecipitation (Figure 4B, lanes 1 and 2), and complexes of Bim mRNA bound to immunoprecipitated Hsc70 formed less efficiently in the presence of IL-3 than in its absence (Figure 4C). In contrast, binding of c-*fos* mRNA to immunoprecipitates did not vary in the presence or absence of IL-3 (right panel).

Immunoblots were used to test whether cochaperones that associate with Hsc70 (Bag family proteins, CHIP, Hip, and Hsp40, reviewed in Mayer and Bukau [2005]) mediate the IL-3 sensitivity of Hsc70 binding to Bim mRNA. Bag-1, -2, and -4 and CHIP, Hip, and Hsp40 were all detected in Baf-3 cell lysates. Of these, only Bag-4 steady-state levels were higher in IL-3-treated cells (Figure 4B, top row). When immunoblots of Hsc70 immunoprecipitates were analyzed with the same antibodies, all cochaperones except Bag-2 were detected (second row). Furthermore, the relative amounts of Bag-4 and CHIP that coprecipitated with Hsc70 increased in IL-3-treated cells, while those of Hsp40 and Hip decreased. By comparing the cochaperone signal strengths of Hsc70-bound or -unbound fractions, we estimate that 90% of Bag-4 coprecipitated with Hsc70, while only less than 10% of CHIP, Hip, or Hsp40 was present in Hsc70 immunocomplexes.

A cytosol-free system was used to test whether CHIP, Hip, or Hsp40 affect the RNA binding potential of Hsc70. In immunoblots with anti-Hsc70, the signal from purified Hsc70 bound to Bim mRNA-coated beads did not exceed background; however, addition of purified Hsp40 (DjB1) or Hip to the RNA binding reactions enhanced Hsc70 binding more than 4-fold (Figure 4D). Addition of both Hsp40 and Hip to the reactions did not further increase Hsc70 binding affinity to RNA, suggesting that these cochaperones enhance the stability of Hsc70 binding to RNA through common molecular mechanisms. In contrast, CHIP did not increase the recovery of Hsc70 from the RNA column but reversed Hsp40 and Hip stabilization of Hsc70-Bim mRNA complexes. These results support evidence that cochaperones bound to Hsc70 regulate the RNA binding potential of the Hsc70-protein complex.

Bag-4 and Hsp40 Control Baf-3 Cell Survival by Regulating Bim Expression

Baf-3 cell lines that overexpress Bag-4 were established. In one representative clone #17, steady-state levels of Bag-4 protein levels were maintained, in contrast to parent Baf-3 cells, in which Bag-4 declined after IL-3 starvation (Figure 4E). Extracts made from clone #17 cells cultured in the absence of IL-3 also induced more rapid deadenylation and degradation of Bim mRNA in vitro than control cell extracts (Figure 5A). Induction of Bim mRNA by IL-3 starvation is suppressed in Bag-4-overexpressing cells (Figures 5B and 5C). Bim protein induction was also attenuated (Figure 5D), although not as prominently as in Hsc70 knockdown cells (Figures 3D–3F). Consistent with these data, Bag-4-overexpressing cells continued to divide and survived longer than Baf-3 parent cells in IL-3-free medium (Figure 5E).

Steady-state levels of Bag-4 mRNA from early undifferentiated hematopoietic progenitors (Sca-1$^+$c-Kit$^+$Lin$^-$ from mouse primary bone marrow cultures) that proliferate in a SCF- and TPO-dependent manner (Kuribara et al., 2004) were measured by using qRT-PCR. Bag-4 mRNA levels declined when these cells were deprived of cytokines (Figure 4F), suggesting that cytokine-mediated survival of progenitor cells may involve Bag-4 control of mRNA stability.

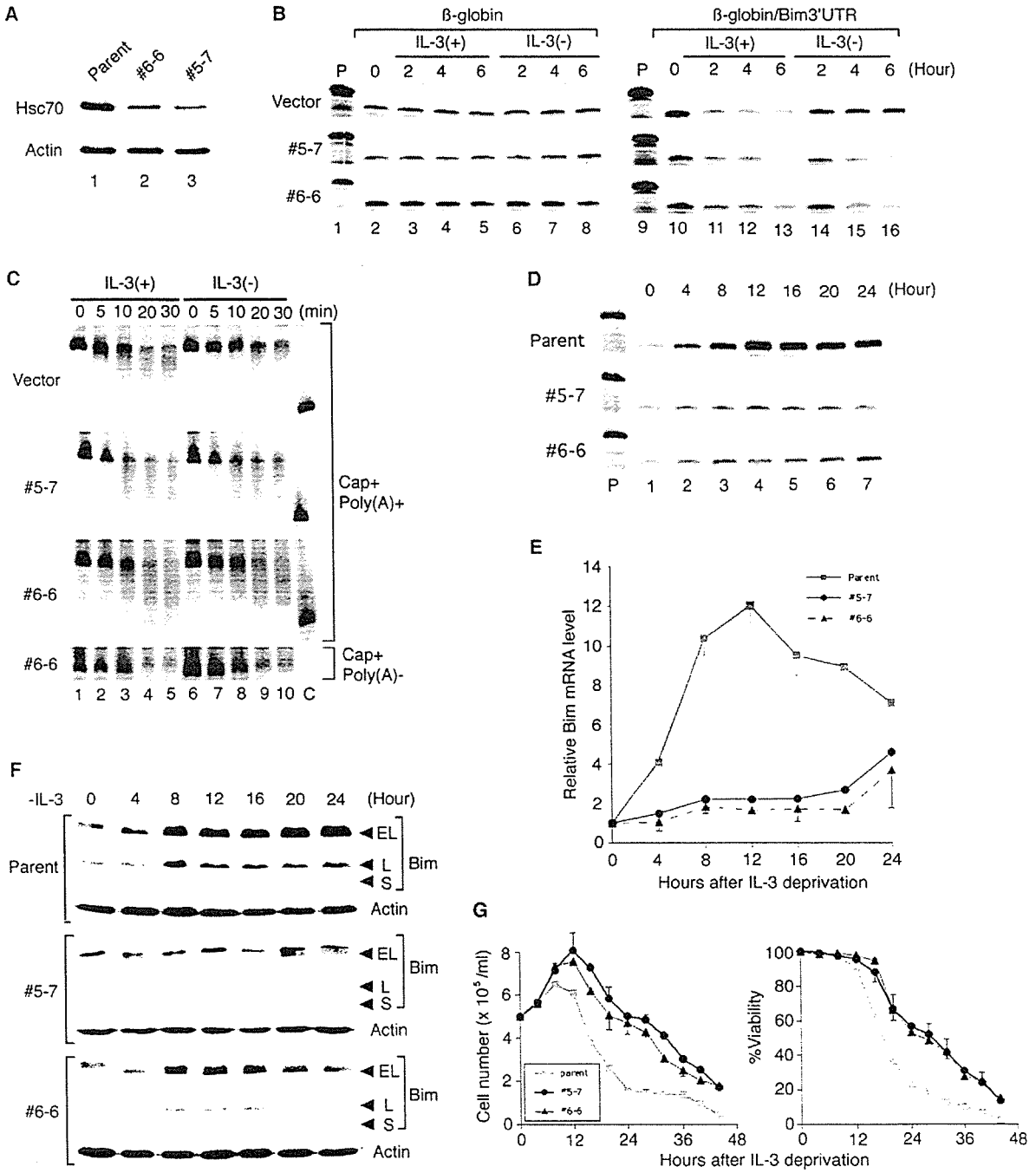

Figure 3. Effects of Hsc70 on mRNA Stability

(A) Immunoblot analysis of lysates from parent Baf-3 cells and representative lines expressing shRNAs that target different sequences in Hsc70 mRNA with Hsc70 or β-actin antibody.

(B) The stabilities of human β-globin mRNA or a β-globin/Bim (3′UTR) fusion mRNAs expressed transiently in two Hsc70 knockdown clones (and control cells with the piGENE-mU6 vector) cultured either in the presence or absence of IL-3. Message levels were measured using RPA.

(C) RNA-stability assay in vitro. Cytosol preparations from two Hsc70 knockdown clones and the negative control cells cultured in the presence or absence of IL-3 were incubated for indicated periods with radiolabeled and capped Bim mRNA with (top and middle panels) or without (bottom panel) a poly(A) tail of 100 residues.

(D–G) Parental Baf-3 cells and two Hsc70 knockdown lines were cultured without IL-3 for indicated periods. Bim mRNA expression was measured using RPA (D) or qRT-PCR (E). Bim and control β-actin protein expression (F), cell number (left), and viability (right) (G) are also shown. The mean and SD of three independent experiments are shown (E and G).

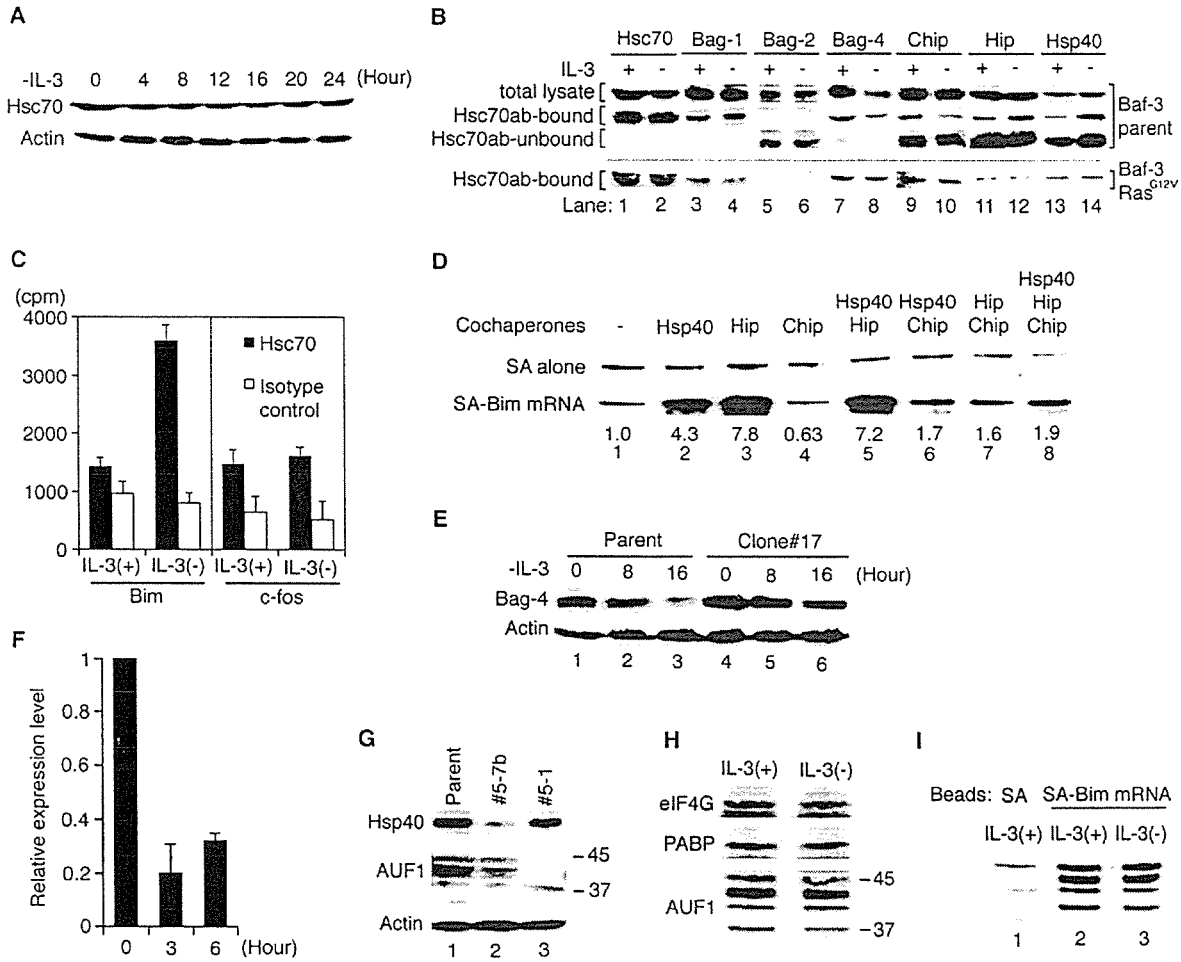

Figure 4. Cochaperones and RNA Binding Proteins Binding to Hsc70

(A) Hsc70 and β-actin protein levels in Baf-3 cells cultured without IL-3 for the times indicated.

(B) Cell extracts prepared from parent Baf-3 cells (upper three panels) or cells expressing Ras^{G12V} (bottom panels) cultured in the presence or absence of IL-3. Levels of individual proteins visualized by immunoblots of Baf-3 lysates with specific cochaperone antibodies marked above (top panels). Following immunoprecipitation, Hsc70 antibody-bound (upper middle and bottom panels) and Hsc70 antibody-unbound (lower middle panels) proteins were detected by immunoblotting. Equivalent cell numbers were analyzed.

(C) Immunoprecipitates with either Hsc70 antibodies or isotype control immunoglobulins were incubated with radiolabeled Bim (left) or c-*fos* (right) mRNAs. The amount of RNA bound to the beads was measured using a scintillation counter. The mean ± SD of three independent experiments is shown.

(D) Streptavidin beads (SA) alone or preincubated with biotinylated Bim mRNA (SA-Bim mRNA) were mixed with purified Hsc70 protein alone (lane 1) or Hsc70 with the cochaperones indicated above. Bead-bound Hsc70 protein was detected by immunoblot analysis. For each lane, the quantity of Hsc70 bound to SA-Bim mRNA relative to lane 1 is shown below.

(E) Parental Baf-3 cells and cells overexpressing Bag-4 (Clone #17) were cultured without IL-3 for the indicated periods. Immunoblot analyses with Bag-4 and β-actin antibodies are shown.

(F) Relative levels of Bag-4 mRNA were measured by qRT-PCR in murine early hematopoietic progenitors ($Sca1^+cKit^+Lin^-$) cultured in SCF- and TPO-free medium for the indicated periods. The mean and SD of three independent experiments are shown.

(G) Immunoblot analysis of Hsp40, AUF1, and β-actin by using lysates from parent Baf-3 cells or from representative lines #5-7b and #5-1, which express shRNAs targeting Hsp40 or AUF1 mRNA, respectively.

(H) Cytosol extracts of Baf-3 cells cultured with or without IL-3 were used in immunoprecipitations with Hsc70 antibody and then analyzed in immunoblots with antibodies against eIF4G, PABP, or AUF1.

(I) Streptavidin beads (SA) alone (lane 1) or those incubated with biotinylated Bim mRNA (SA-Bim mRNA; lanes 2 and 3) were mixed with cytosol from Baf-3 cells cultured with or without IL-3. Bead-bound AUF1 protein was detected by immunoblot analysis.

Hsp40 (DjB1) protein levels were reduced in Baf-3 clones expressing an Hsp40-specific shRNA (clone #5-7b, Figure 4G). In in vitro RNA decay assays, these cells showed mild enhancement of Bim mRNA deadenylation (Figure 5A), which correlates well with the mild suppression of Bim mRNA induction that occurs with IL-3

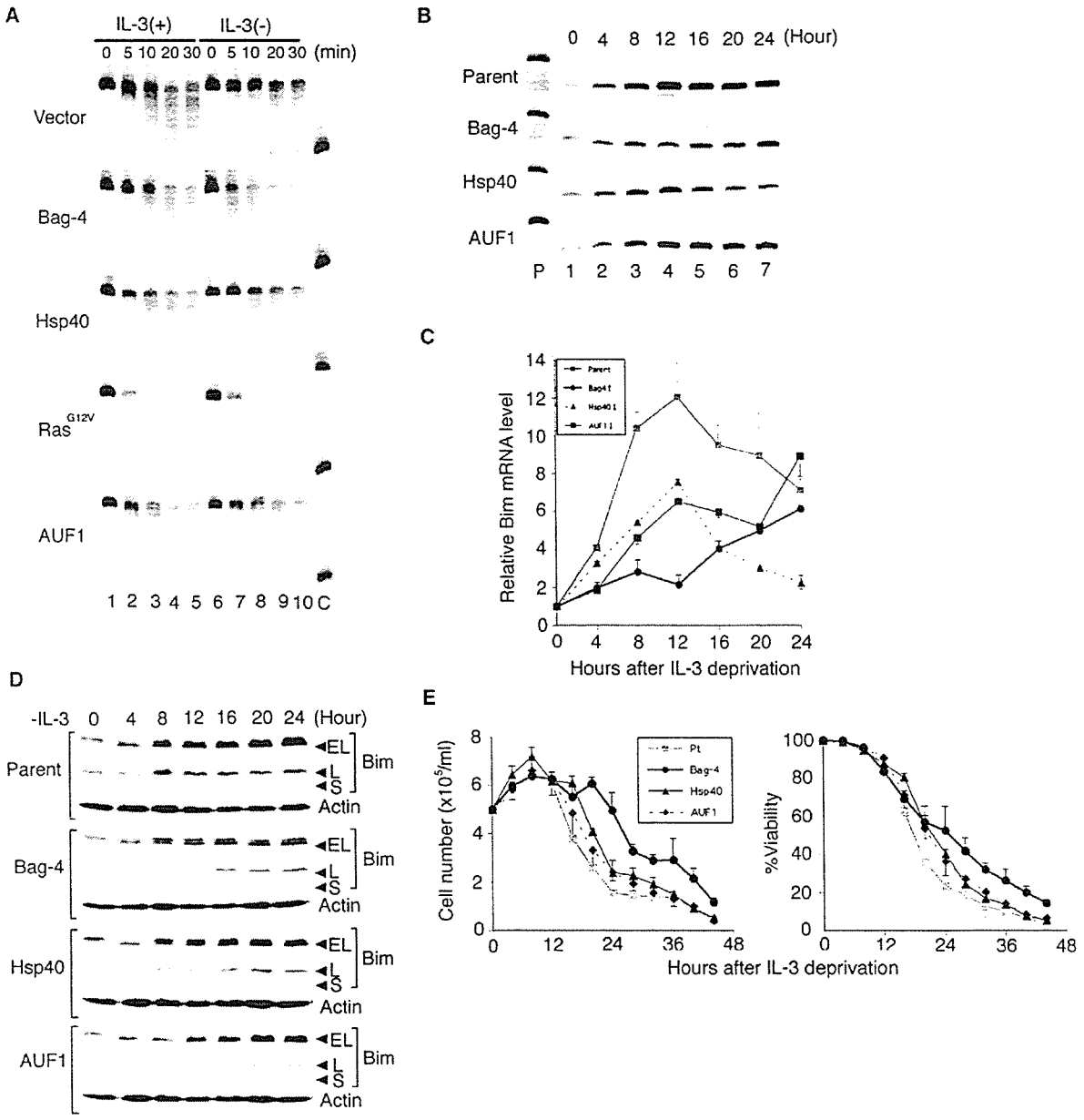

Figure 5. Effects of Hsc70 Binding Proteins on Bim Expression

Control Baf-3 cells transfected with the empty piGENE-mU6 vector, Bag-4-overexpressing clone #17, Hsp40 knockdown clone #5-7b, Ras^{G12V}-overexpressing cells, and AUF1 knockdown clone #5-1 were cultured with or without IL-3.

(A) RNA-stability assays in vitro using radiolabeled and capped Bim mRNA with a poly(A) tail of 100 residues.

(B–E) Cells were cultured without IL-3 for the times indicated above. Bim mRNA expression was analyzed using (B) ribonuclease protection assays, as well as (C) qRT-PCR. (D) Bim and β-actin protein expression. (E) Cell number (left) and viability (right). The mean and SD of three independent experiments are shown (C and E).

starvation (Figures 5B and 5C). However, Bim protein levels did not change (Figure 5D), and cell survival in the absence of IL-3 did not improve significantly (Figure 5E). Attempts to establish Baf-3 cell lines that overexpress CHIP or express Hip shRNA were not successful.

Hsp70 Fails to Substitute for Hsc70 as a Bim mRNA Stabilizer

Despite previous reports of heat-inducible Hsp70 binding to AREs (Henics et al., 1999; Zimmer et al., 2001; Wilson et al., 2001), Hsp70 was not detected among proteins

bound to Bim RNA on columns exposed to lysates of Baf-3 cells grown in the presence or absence of IL-3 (Figure 2D). To determine whether this is caused by the low expression level of Hsp70 in Baf-3 cells (Figure 6A, lanes 1 and 2) or inability of Hsp70 to bind to Bim mRNA, we tested Hsp70's RNA binding potential directly in a cytosol-free system. We detected no significant binding of Hsp70 to Bim mRNA either alone or in the presence of Hsp40 and Hip (Figure 6B). UV-crosslinking assays showed that recombinant Hsp70 with Hsp40 and Hip bound to c-*fos* mRNA, but not to Bim mRNA (Figure 6C). Potential of Hsp70 to stabilize Bim mRNA in the absence of Hsc70 was tested by using Baf-3 cells with Hsc70 levels reduced by shRNA expression (clone #6-6) and also expressed Hsp70 constitutively (#6-6+Hsp70 #1 and #3, Figure 6A). In in vitro mRNA decay assays, lysates from these clones grown in the presence or absence of IL-3, showed poor stabilization of Bim mRNA (Figure 6D). Consistent with these results, there was no increase in Bim protein levels in IL-3-starved cells (Figure 6E), and the survival of these lines was prolonged in the absence of IL-3 relative to Baf-3 parent cells (Figure 6F). These results indicate that Hsp70 does not bind to Bim mRNA and cannot substitute for Hsc70 in the stabilization of Bim mRNA.

Ras^{G12V} Regulates the Binding Potentials of Cochaperones to Hsc70 and Destabilizes Bim mRNA

Previous reports established that Ras-activated pathways play a critical role in the transduction of survival signals from cytokine receptors (reviewed by Inaba [2004]). When starved for IL-3, Baf-3 cells expressing constitutively active Ras (Ras^{G12V}) show no induction of Bim mRNA, and cells live indefinitely in IL-3-free medium. In in vitro Bim mRNA decay assays, Bim mRNA was rapidly deadenylated in extracts of Baf-3 cells expressing Ras^{G12V} in the absence or presence of IL-3 (Figure 5A).

To investigate what components may be involved in this extremely rapid mRNA decay, the Hsc70/cochaperone complex formed in Baf-3 cells expressing Ras^{G12V} was examined by immunoblot analysis of Hsc70 immunoprecipitates with cochaperone-specific antibodies. Levels of cochaperones associated with Hsc70 were the same in Baf-3 cells grown in the absence or presence of IL-3 (Figure 4B, bottom panels), and Bag-4, CHIP, and Hsp40 levels were similar to those observed in parent Baf-3 cells cultured with IL-3. One possible contribution to the very rapid decay of Bim mRNA may be the levels of Hsc70-bound Hip protein, which were reduced in cells expressing Ras^{G12V} relative to parent cells cultured with IL-3.

Hsc70 Forms a Complex with eIF4G, PABP, and AUF1

Hsc70 interacts with AUF1, an ARE binding protein that regulates RNA stability and forms a ternary complex with eIF4G/eIF4E (translation initiation factors that bind to the cap) and poly(A) binding protein (PABP) (Laroia et al., 1999; Grosset et al., 2000). In coimmunoprecipitation assays from extracts of Baf-3 cells cultured with or without IL-3, there were similar levels of eIF4G, PABP and four alternative spliced isoforms of AUF1 (p37, p40, p42, and p45) in complex with Hsc70 (Figure 4H).

Unlike Hsc70 (Figure 2), the recovery of AUF1 with Bim mRNA-coated beads did not vary in cytosol extracts prepared from Baf-3 cells cultured in the presence or absence of IL-3 (Figure 4I). The role of AUF1 in Bim mRNA stability was investigated in Baf-3 cells expressing AUF1 shRNA. Although all forms of AUF1 except p37 were less abundant in clone #5-1 (Figure 4G), AUF1 downregulation had little or no effect on Bim mRNA decay (Figure 5A), steady-state levels of Bim mRNA (Figures 5B and 5C) or Bim protein (Figure 5D), or cell growth and survival in the absence of IL-3 (Figure 5E). These results suggest a limited role for AUF1 in the regulation of Bim mRNA stability.

DISCUSSION

In earlier studies, we and others demonstrated that regulation of Bim and p27 steady-state mRNA levels by cytokines contributes to homeostasis of blood cell number. Here we demonstrate that cytokines shorten the half-life of Bim mRNA by reducing the RNA binding affinity of Hsc70, an mRNA-stabilizing factor. We propose the following model for cytokine-mediated control of Bim mRNA (Figure 7). In the presence of IL-3, Hsc70 protein that is associated with Bag-4 and CHIP has little RNA binding potential. As a result, Bim mRNA is more likely to be bound by a RNA-destabilizing factor(s), which targets Bim mRNA for degradation by ribonucleases. In the absence of IL-3, Hsc70 binds preferentially to Hsp40 and Hip. The association of this complex (with eIF4G and PABP) with Bim mRNA protects it from ribonucleases. Aspects of this model also apply to the cytokine-dependent regulation of p27 mRNA.

AUF1 is a target of ubiquitin-protease pathways that contributes to the rapid turnover of ARE-containing mRNAs (Laroia et al., 1999). As a component of the Hsc70 complex (Figure 4H) that was detected in Baf-3 cells by Bim RNA-affinity chromatography (Figure 4I), AUF1 is a candidate Bim mRNA destabilizer. However, interactions between AUF1 and Hsc70 or Bim mRNA did not change by IL-3 (Figures 4H and 4I). Moreover, shRNA-mediated downregulation of AUF1 did not alter Bim mRNA stability (Figures 5A–5C). Among the four alternatively spliced variants, $p37^{AUF1}$ is the major ubiquitinated isoform that contributes to rapid degradation of mRNA (Laroia and Schneider, 2002; Sarkar et al., 2003). Because we failed to downregulate this isoform (Figure 4G), we overexpressed $p37^{AUF1}$ in Baf-3 cells, and again little effect was observed (data not shown). These findings support a model in which an mRNA-destabilization factor(s) other than AUF1 plays a critical role in the rapid decay of Bim mRNA in IL-3-treated Baf-3 cells.

We demonstrated previously that activation of Ras pathways is essential for the downregulation of Bim mRNA and the long-term survival of Baf-3 cells (Kuribara

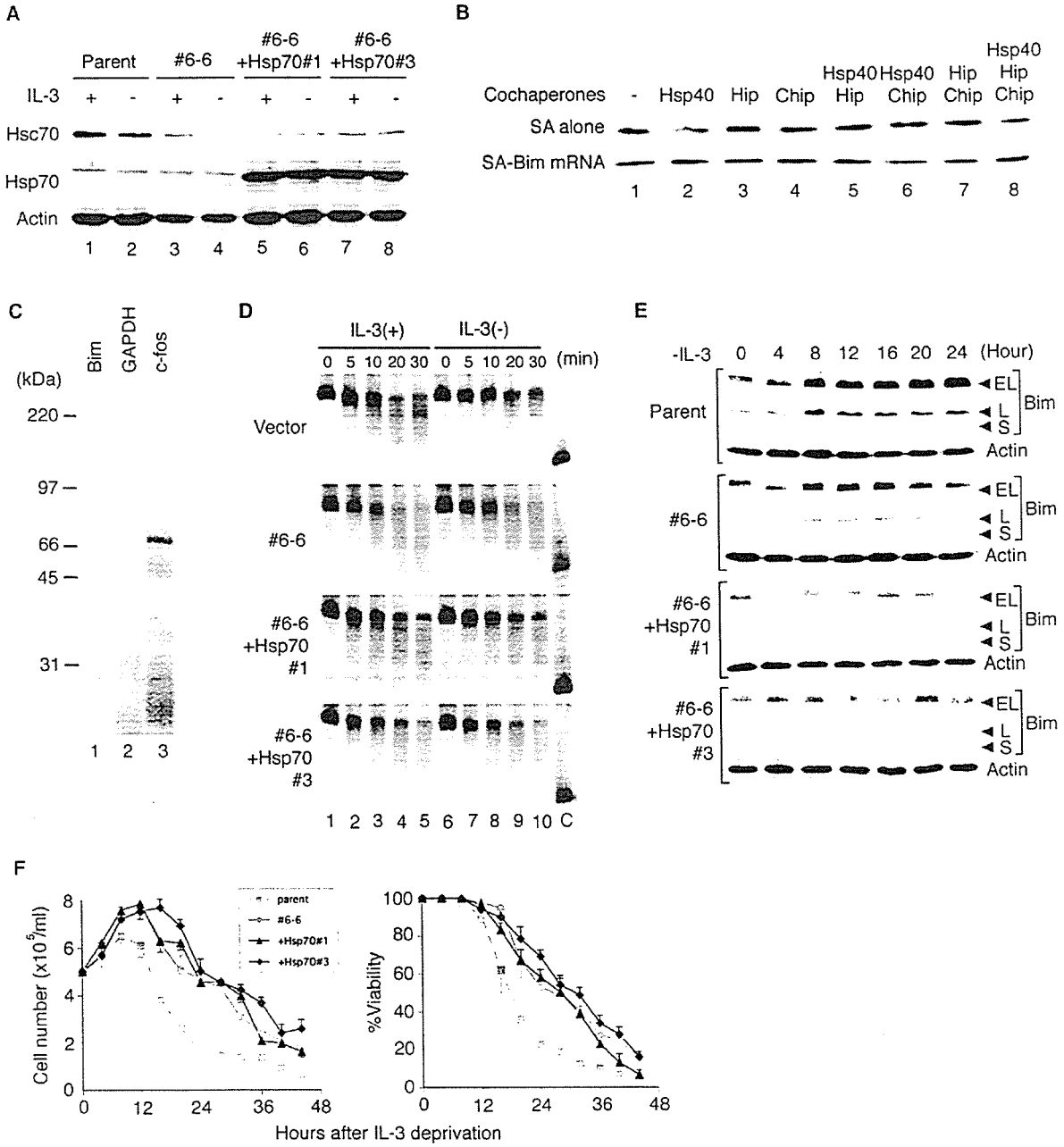

Figure 6. Inability of Hsp70 to Stabilize Bim mRNA

(A) Immunoblot analysis of Hsc70 (top panel), Hsp70 (middle panel), and β-actin (bottom panel) in lysates from parent Baf-3 cells, Hsc70 knockdown clone #6-6, and two representative lines from #6-6 that express Hsp70 constitutively.

(B) Streptavidin beads (SA) alone (top panel) or preincubated with biotinylated Bim mRNA (SA-Bim mRNA; bottom panel) were mixed with purified Hsp70 protein alone (lane 1) or with the cochaperones indicated above. Bead-bound Hsp70 protein was detected by immunoblot analysis.

(C) UV-crosslinking assay. Mixtures of recombinant Hsp70, Hsp40, and Hip were incubated with radiolabeled Bim, GAPDH, or *c-fos* mRNA.

(D–F) Parent Baf-3 cells, clone #6-6, and two clones from #6-6 expressing Hsp70 were cultured with or without IL-3 for indicated periods. RNA stability assay in vitro, using capped Bim mRNA with a poly(A) tail (D), Bim and β-actin protein expression (E), and the mean and SD of cell number (left) and viability (right) in three independent experiments (F) are shown.

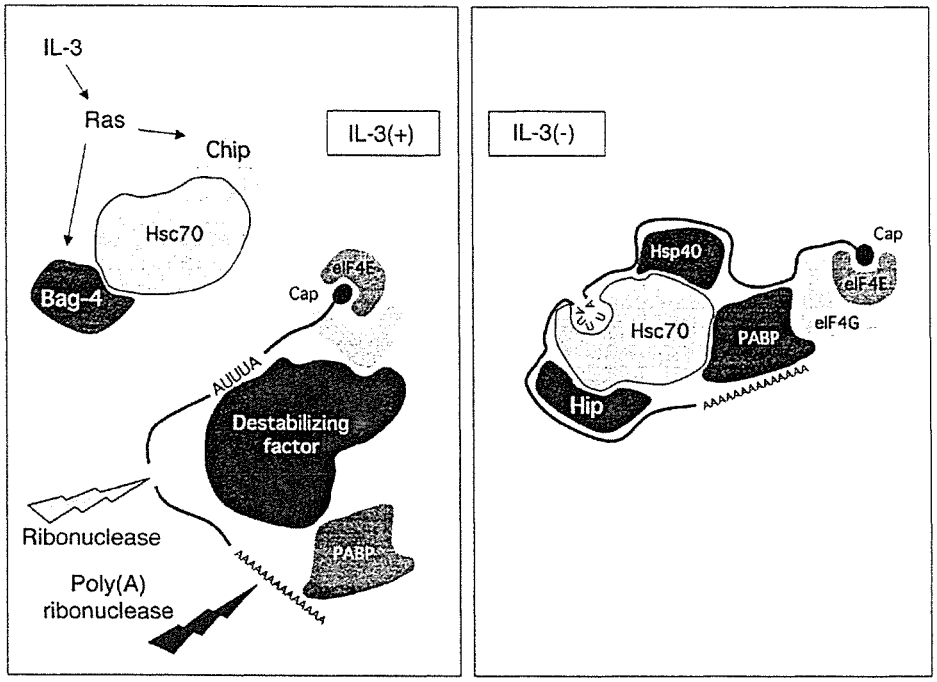

Figure 7. Model for the Cytokine-Dependent Regulation of mRNA Stability
In the presence of IL-3, Hsc70 associated with Bag-4 and CHIP has a low affinity for RNA. Bim mRNA, which preferentially binds to RNA destabilizing factor(s), is a target for ribonucleases. In the absence of IL-3, an Hsc70/Hsp40/Hip complex associated with eIF4G and PABP forms a high-stability complex with Bim mRNA that protects it from ribonucleases.

et al., 1999; Shinjyo et al., 2001). Consistent with these data, induced expression of Ras^{G12V} resulted in extremely rapid decay of Bim mRNA (Figure 5A) and bypassed the requirement for IL-3 as a regulator of Hsc70 binding to Bag-4, CHIP, Hip, or Hsp40 (Figure 4B). Thus, we hypothesize that these cochaperones (and possibly others) function *cooperatively* in responding to cytokine-dependent survival signals by regulating Hsc70's RNA binding potential. Our finding that changes in the steady-state levels of a single cochaperone affect Bim mRNA expression less than downregulation of Hsc70 itself support this hypothesis. We are currently investigating a molecular mechanism(s) by which IL-3 and Ras^{G12V} regulate CHIP, Hip and Hsp40 binding to Hsc70.

Previous reports of the RNA binding potential of Hsc70 and Hsp70, which bind directly to native AREs as well as artificial AUUUA-containing RNAs, illustrate few differences between these two chaperones (Henics et al., 1999; Zimmer et al., 2001; Wilson et al., 2001). In contrast, we found that, unlike Hsc70, Hsp70 binds well to the c-*fos* ARE and only weakly to Bim mRNA in the presence of Hsp40 and/or Hip (Figures 6B and 6C). Hsp70 also failed to substitute for Hsc70 as a Bim mRNA stabilizer (Figures 6D–6F). Theologically, any model involving Hsp70 binding directly to Bim mRNA would promote cell killing instead of protecting cells in stressful conditions.

Hsp70 family chaperones share common structural motifs including a 45 kDa N-terminal ATPase domain and a 23 kDa C-terminal substrate binding domain composed of a β sandwich and α helix subdomains (Zhu et al., 1996). Although Hsp70 and Hsc70 amino acids are nearly 90% identical in the ATPase domain and β sandwich subdomain, identity in the α helix subdomain is only 65% identical. The ATPase domain has been determined to be sufficient for ARE binding, but the substrate binding domain is required for RNA binding fidelity and sequence preference (Zimmer et al., 2001). Thus, divergence in the α helix subdomains of Hsc70 and Hsp70 could target the specificities of these proteins binding to Bim and c-*fos* mRNAs, respectively. Because the AREs of Bim, p27, and c-*fos* are all classified as "WAUUUAW and U-rich region" motifs (W stands for A or U) (reviewed in Wilusz et al. [2001]), it is conceivable that α helix subdomains may distinguish *cis* elements other than AUUUA within AREs that are currently unidentified.

Although Hsp70's α helix subdomain is likely to play an important role in gene-specific RNA binding of chaperones, differences in the protein band patterns resulting from Bim/p27, GAPDH, and c-*fos* RNA-affinity chromatography and UV-crosslinking assays (Figures 2A and 2F) suggest contributions of other 3′UTR binding proteins. It should also be noted that although AREs play a critical role as protein docking sites, non-ARE flanking sequences may also function as *cis*-acting regulatory elements that further specify the binding potential of Hsc70 to AREs. A recent report of CA repeats that mediate constitutive

degradation of Bcl-2 mRNA (Lee et al., 2004) suggests involvement of non-ARE sequences in the control of mRNA stability.

Because Bim plays a critical role in the regulation of hematopoietic cell number (Bouillet et al., 1999), altered regulation of Bim could be involved in leukemogenesis. Negative regulation of Bim by the Bcr-Abl chimeric kinase has been shown to contribute to an increase in white blood cell and hematopoietic progenitor counts in the chronic phase of chronic myelogenous leukemia (CML) (Kuribara et al., 2004; Aichberger et al., 2005). At least part of the inhibition of leukemic blast proliferation provided by antileukemic drugs such as imatinib mesylate or AMN107 (which target Bcr-Abl kinase) is due to increased levels of Bim protein (Kuribara et al., 2004; Aichberger et al., 2005; Fiskus et al., 2006). Because negative regulation of Bim by Bcr-Abl may be mediated by Hsc70 and associated cochaperones, our laboratory endeavors to understand the formation and regulation of this complex as a means to identify new molecular targets for antileukemic drugs.

EXPERIMENTAL PROCEDURES

Cells and Cell Culture

IL-3-dependent cells were cultured as described previously (Shinjyo et al., 2001). The piGENE-mU6 vector (Miyagishi et al., 2004) was used for expression of shRNAs with sequences targeting Hsc70#5, UGAGGGAAUUGACUUCUAUAC; Hsc70#6, UGAUGCUGUUGUUCA GUCUGA; Hsp40#5, GUGGAGACCUUGUUAUCGAGU; or AUF1#5, ACAAUGUUGGUCUUAGUAAAU. Bag-4 and Hsp70 overexpression lines were established by standard procedures (Shinjyo et al., 2001). At least three independent clones were isolated and analyzed. Baf-3 cells expressing Ras^{G12V} were a gift from Dr. Atsushi Miyajima. Murine undifferentiated early hematopoietic progenitors ($Sca\text{-}1^{+}c\text{-}Kit^{+}Lin^{-}$) were isolated and cultured as previously described (Kuribara et al., 2004).

Measurements of mRNA Stability

mRNA stability in vivo was measured using the Tet-inducible expression system as previously described (Xu et al., 1998). Native and hybrid human β-globin mRNAs were detected by RPA or by qRT-PCR with primers 5′-GGGATCTGTCCACTCCTGATGCTG-3′ in exon 2 and 5′-ATGGGCCAGCACACAGACCAGCAC-3′ in exon 3. Half-lives of in vitro-synthesized mRNAs incubated with cytosolic (S100) cell extracts were analyzed as described previously (Ford and Wilusz, 1999). Target mRNAs included the Bim 3′UTR region conserved between human and mouse, or the complete 3′UTRs of p27 and c-*fos*. Short target mRNA sequences were as follows: Bim, UAACUUGUAG AGAUGUUGUAUAUUUAUUUUCCGCUUAUUUAAAUGUCUUAAGUU CUUGAAA; p27, AAAAUUAUACUAACUUAUUUAUGUUAAAAAGAG AUUUUUUUUUAAUCUAGACAAUAUACAA; and GAPDH, CCCUGG ACCACCCACCCCAGCAAGGACACUGAGCAAGAGAGGCCCUAUCC CAACUCGGCCC. Radiolabeled, capped (^{7Me}GpppG) mRNAs synthesized in vitro with or without a 100 bp poly(A) tail were incubated at 37°C with S100 extracts. Signals from mRNAs resolved on 5% acrylamide gels containing 7 M urea were quantified using a Bas3000 phosphoimager (Fuji, Tokyo, Japan).

Enrichment and Identification of RNA Binding Proteins

RNA-affinity chromatography was performed as described (Skalweit et al., 2003). Briefly, biotinylated mRNAs encoding the 3′UTR of Bim, GAPDH, p27, or c-*fos* mRNA and bound to streptavidin-coated agarose beads were exposed to S100 extracts for 45 min at 4°C and then for 15 min at room temperature. Protein-bound beads were washed gently (150 mM KCl, 1.5 mM $MgCl_2$, 10 mM Tris [pH 7.5], 0.5 mM DTT). Bound proteins were then released by boiling in SDS sample buffer, resolved by SDS-PAGE, and visualized by silver staining or immunoblot analysis. Protein bands of interest were recovered and analyzed using a matrix-assisted laser desorption/ionization time-of-flight (MALDI-TOF/TOF) tandem mass spectrometer (Ultraflex, Bruker, Bremen, Germany).

In Vitro RNA Binding Assay

Hsc70 protein complexes, isolated and eluted from an Hsc70 antibody (1B5, Stressgen, Victoria, Canada) bound to protein G beads, were incubated with in vitro-synthesized radiolabeled mRNA in RNA binding buffer (10 mM MOPS [pH 7.2], 50 mM KCl, 3 mM $MgCl_2$, 0.5 mM ATP, 2 mM DTT) containing RNase OUT (Invitrogen, Carlsbad, California) at 37°C for 30 min. After washing, bead-bound RNA was quantified using a scintillation counter. For cytosol-free RNA binding assays, 10 μg of in vitro-synthesized biotinylated Bim mRNA bound to streptavidin-coated beads was incubated with 500 ng Hsc70 (with or without an equimolar concentration of Hsp40, Hip, or CHIP) in RNA binding buffer at 4°C for 45 min and then at room temperature for 15 min. After washing the beads, bound proteins were released by boiling in SDS sample buffer and were subjected to immunoblot analysis.

RNA gel retardation assays were performed as described (Mahtani et al., 2001). Briefly, Hsc70 (with or without Hsp40 and/or Hip) were preincubated with or without 1 μl of Hsc70 (SPA-816, Stressgen) or Hsp40 antiserum for 30 min on ice. Radiolabeled RNA probe (derived from the human Bim 3′UTR, 5′-UCUGUGUGAUGUGUCCUACUGU UUCAUAAUGCUGUAACUUGUAGAAAUAUUGUAUAUUUAUUUUCU GCUUAUUUAAUGUCUUAAUUUCUGAAA-3′) in RNA binding buffer (20 mM HEPES [pH 7.6], 3 mM $MgCl_2$, 40 mM KCl, 2 mM DTT, and 5% glycerol), RNase T1 (25 U/ml), and heparin sulfate (5 mg/ml) were added, and the mixture was incubated on ice for 20 min. The resulting binding reactions were resolved by electrophoresis on a nondenaturing 4% polyacrylamide gel run at 150 V for 3 hr at 4°C.

UV-crosslinking assay was performed as described (Chen et al., 2000) with modification. Mixtures of recombinant proteins or cytoplasmic extracts (20 μg protein) were incubated with ^{32}P-labeled RNA (0.5 ng = 2 × 10^5 cpm) at room temperature for 20 min in 10 μl of RNA binding buffer containing 1 μg heparin. Reaction mixtures were transferred to a 96-well plate and irradiated for 10 min on ice with a UV Stratalinker (Invitrogen) at a distance of 5 cm. Unbound RNA was then digested with RNase A (200 ng) for 10 min at 37°C, and samples were resolved by SDS-PAGE (10%). Probes were as follows: for Bim or GAPDH, the same as used in gel retardation assays or in vitro mRNA decay assays, respectively; for c-*fos*, 5′-UUUUAUUGUGUUUU UAAUUUAUUUAUUAAGAUGGAUUCUCAGAUAUUUAUAUUUUUAU UUUAUUUUUUU-3′.

Other Experimental Procedures and Reagents

qRT-PCR was performed with exon 1-exon 2 primer sets: 5′-AATGTCTGACTCTGATTCTCGGAC-3′ and 5′-TCTCAGCAGGCTGC AATTGTCCAC-3′ for Bim and 5′-GCAGGTGGCGATGGCTACTAC CCC-3′ and 5′-CCATTTGCATAAGAATTCAGGCTC-3′ for Bag-4, and 28S ribosomal RNA as an internal control (Kuribara et al., 2004). Antibodies included anti-actin (1378 996, Roche, Mannheim, Germany); anti-AUF1 (07-260) and -SODD (Bag-4, 07-092) from Upstate Cell Signaling Solutions (Lake Placid, New York); anti-Bag-1 (FL-274), -Hsc70 (B-6), and -p27 (C-19) from Santa Cruz Biotechnology (Santa Cruz, California); anti-Bag-2 (Oxford Biotechnology, Oxfordshire, United Kingdom); Chip (Ab-1, Oncogene Research Products (San Diego, California); anti-eIF4G1 (BL896, Bethyl laboratories, Montgomery, Texas); and anti-Hip (SPA-766), -Hsp40 (SPA-400), and -Hsp70 (C92F3A-5) from Stressgen. A rabbit anti-PABP was raised against a GST-mouse PABP (aa 213–422) fusion protein, and anti-Bim antibodies were described elsewhere (Shinjyo et al., 2001). Recombinant Hsc70, Hsp70, and Hsp40 (DjB1) proteins were from Stressgen. Hexameric

His-tagged mouse Hip protein was expressed in *E. coli* using the pQE-80L vector (Qiagen, Hilden, Germany) and purified using Ni-NTA beads. Mouse CHIP protein was synthesized as a GST fusion and cleaved by thrombin.

ACKNOWLEDGMENTS

This work was supported by Grants-in-Aid for Scientific Research from the Ministry of Education, Culture, Sports, Science, and Technology of Japan.

Received: August 8, 2006
Revised: November 5, 2006
Accepted: December 12, 2006
Published: January 11, 2007

REFERENCES

Aichberger, K.J., Mayerhofer, M., Krauth, M.T., Vales, A., Kondo, R., Derdak, S., Pickl, W.F., Selzer, E., Deininger, M., Druker, B.J., et al. (2005). Low-level expression of proapoptotic Bcl-2-interacting mediator in leukemic cells in patients with chronic myeloid leukemia: role of BCR/ABL, characterization of underlying signaling pathways, and reexpression by novel pharmacologic compounds. Cancer Res. *65*, 9436–9444.

Akiyama, T., Bouillet, P., Miyazaki, T., Kadono, Y., Chikuda, H., Chug, U., Fukuda, A., Hikita, A., Seto, H., Okada, T., et al. (2003). Regulation of osteoclast apoptosis by ubiqutination of proapoptotic BH3-only Bcl-2 family member Bim. EMBO J. *22*, 6653–6664.

Birkenkamp, K.U., and Coffer, P.J. (2003). Regulation of cell survival and proliferation by the FOXO (Forkhead box, class O) subfamily of Forkhead transcription factors. Biochem. Soc. Trans. *31*, 292–297.

Bouillet, P., Metcalf, D., Huang, D.C.S., Tarlinton, D.M., Kay, T.W.H., Koentgen, F., Adams, J.M., and Strasser, A. (1999). Proapoptotic Bcl-2 relative Bim required for certain apoptotic responses, leukocyte homeostasis, and to preclude autoimmunity. Science *286*, 1735–1738.

Chen, C.Y., Gherzi, R., Andersen, J.S., Gaietta, G., Jurchott, K., Royer, H.D., Mann, M., and Karin, M. (2000). Nucleolin and YB-1 are required for JNK-mediated interleukin-2 mRNA stabilization during T-cell activation. Genes Dev. *14*, 1236–1248.

Dijkers, P.F., Medemadagger, R.H., Lammers, J.J., Koenderman, L., and Coffer, P.J. (2000a). Expression of the proapoptotic bcl-2 family member bim is regulated by the forkhead transcription factor FKHR-L1. Curr. Biol. *10*, 1201–1204.

Dijkers, P.F., Medema, R.H., Pals, C., Banerji, L., Thomas, N.S., Lam, E.W., Burgering, B.M., Raaijmakers, J.A., Lammers, J.W., Koenderman, L., et al. (2000b). Forkhead transcription factor FKHR-L1 modulates cytokine-dependent transcriptional regulation of p27(KIP1). Mol. Cell. Biol. *20*, 9138–9148.

Duttagupta, R., Vasudevan, S., Wilusz, C.J., and Peltz, S.W. (2003). A yeast homologue of Hsp70, Ssa1p, regulates turnover of the MFA2 transcript through its AU-rich 3′ untranslated region. Mol. Cell. Biol. *23*, 2623–2632.

Fero, M.L., Rivkin, M., Tasch, M., Porter, P., Carow, C.E., Firpo, E., Polyak, K., Tsai, L.H., Broudy, V., Perlmutter, R.M., et al. (1996). A syndrome of multiorgan hyperplasia with features of gigantism, tumorigenesis, and female sterility in p27(Kip1)-deficient mice. Cell *85*, 733–744.

Fiskus, W., Pranpat, M., Bali, P., Balasis, M., Kumaraswamy, S., Boyapalle, S., Rocha, K., Wu, J., Giles, F., Manley, P.W., et al. (2006). Combined effects of novel tyrosine kinase inhibitor AMN107 and histone deacetylase inhibitor LBH589 against Bcr-Abl expressing human leukemia cells. Blood *108*, 645–652.

Ford, L.P., and Wilusz, J. (1999). An in vitro system using HeLa cytoplasmic extracts that reproduces regulated mRNA stability. Methods *17*, 21–27.

Freeman, R.S., Burch, R.L., Crowder, R.J., Lomb, D.J., Schoell, M.C., Straub, J.A., and Xie, L. (2004). NGF deprivation-induced gene expression: after ten years, where do we stand? Prog. Brain Res. *146*, 111–126.

Gilley, J., Coffer, P.J., and Ham, J. (2003). FOXO transcription factors directly activate bim gene expression and promote apoptosis in sympathetic neurons. J. Cell Biol. *162*, 613–622.

Grosset, C., Chen, C.-Y.A., Xu, N., Sonenberg, N., Jacquemin-Sablon, H., and Shyu, A.-B. (2000). A mechanism for tranlationally coupled mRNA turnover: interaction between the poly(A) tail and a c-*fos* RNA coding determinant via a protein complex. Cell *103*, 29–40.

Henics, T., Nagy, E., Oh, H.J., Csermely, P., von Gabain, A., and Subjeck, J.R. (1999). Mammalian Hsp70 and Hsp110 proteins bind to RNA motifs involved in mRNA stability. J. Biol. Chem. *274*, 17318–17324.

Hohfeld, J., Minami, Y., and Hartl, F.U. (1995). Hip, a novel cochaperone involved in the eukaryotic Hsc70/Hsp40 reaction cycle. Cell *83*, 589–598.

Hsu, S.Y., Lin, P., and Hsueh, A.J. (1998). BOD (Bcl-2-related ovarian death gene) is an ovarian BH3 domain-containing proapoptotic Bcl-2 protein capable of dimerization with diverse antiapoptotic Bcl-2 members. Mol. Endocrinol. *12*, 1432–1440.

Inaba, T. (2004). Cytokine-mediated cell survival. Int. J. Hematol. *80*, 210–214.

Kuribara, R., Kinoshita, T., Miyajima, A., Shinjyo, T., Yoshihara, T., Inukai, T., Ozawa, K., Look, A.T., and Inaba, T. (1999). Two distinct interleukin-3-mediated signal pathways, Ras-NFIL3(E4BP4) and Bcl-xL, regulate the survival of murine pro-B lymphocytes. Mol. Cell. Biol. *19*, 2754–2762.

Kuribara, R., Honda, H., Matsui, H., Shinjyo, T., Inukai, T., Sugita, K., Nakazawa, S., Hirai, H., Ozawa, K., and Inaba, T. (2004). Roles of Bim in apoptosis of normal and Bcr-Abl-expressing hematopoietic progenitors. Mol. Cell. Biol. *24*, 6172–6183.

Laroia, G., and Schneider, R.J. (2002). Alternate exon insertion controls selective ubiquitination and degradation of different AUF1 protein isoforms. Nucleic Acids Res. *30*, 3052–3058.

Laroia, G., Cuesta, R., Brewer, G., and Schneider, R.J. (1999). Control of mRNA decay by heat shock-ubiquitin-proteasome pathway. Science *284*, 499–502.

Lee, J.H., Jeon, M.H., Seo, Y.J., Lee, Y.J., Ko, J.H., Tsujimoto, Y., and Lee, J.H. (2004). CA repeats in the 3′-untranslated region of bcl-2 mRNA mediate constitutive decay of bcl-2 mRNA. J. Biol. Chem. *279*, 42758–42764.

Ley, R., Balmanno, K., Hadfield, K., Weston, C.R., and Cook, S.J. (2003). Activation of the ERK1/2 signalling pathway promotes phosphorylation and proteasome-dependent degradation of the BH3-only protein Bim. J. Biol. Chem. *278*, 18811–18816.

Luciano, F., Jacquel, A., Colosetti, P., Herrant, M., Cagnol, S., Pages, G., and Auberger, P. (2003). Phosphorylation of Bim-EL by Erk1/2 on serine 69 promotes its degradation via the proteasome pathway and regulates its proapoptotic function. Oncogene *22*, 6785–6793.

Mahtani, K.R., Brook, M., Dean, J.L., Sully, G., Saklatvala, J., and Clark, A.R. (2001). Mitogen-activated protein kinase p38 controls the expression and posttranslational modification of tristetraprolin, a regulator of tumor necrosis factor alpha mRNA stability. Mol. Cell. Biol. *21*, 6461–6469.

Matsui, H., Shinjyo, T., and Inaba, T. (2005). Structure of the human Bim gene and its transcriptional regulation in Baf-3, interleukin-3-dependent hematopoietic cells. Mol. Biol. Rep. *32*, 79–85.

Mayer, M.P., and Bukau, B. (2005). Hsp70 chaperones: cellular functions and molecular mechanism. Cell. Mol. Life Sci. *62*, 670–684.